THE JOURNAL OF PHYSICAL CHEMISTRY C

Article

pubs.acs.org/JPCC

Catalytic Ring Opening of Cycloalkanes on Ir Clusters: Alkyl Substitution Effects on the Structure and Stability of C−C Bond Cleavage Transition States

David W. Flaherty,[†,‡] Alper Uzun,[†] and Enrique Iglesia*[,†]

[†]Department of Chemical Engineering, University of California at Berkeley, Berkeley, California 94720, United States

[‡]Department of Chemical and Biomolecular Engineering, University of Illinois at Urbana−Champaign, Urbana, Illinois 61801, United States

Supporting Information

ABSTRACT: Rates and locations of C−C cleavage during the hydrogenolysis of alkyl-cyclohexanes determine the isomeric products of ring opening and the yield losses from dealkylation. Kinetically relevant transition states for C−C rupture form by sequential quasi-equilibrated dehydrogenation steps that break C−H bonds, form C−metal bonds, and desorb chemisorbed H atoms (H*) from H*-covered surfaces. Activation enthalpies ($\Delta H^{\ddagger}$), entropies ($\Delta S^{\ddagger}$), and the number of H_2(g) formed with transition states are larger for ^{3}C−^{x}C rupture than for ^{2}C−^{2}C or ^{2}C−^{1}C cleavage for all cycloalkane reactants and Ir cluster sizes. ^{3}C−^{x}C rupture transition states bind to surfaces through three or more C atoms, whereas those for less-substituted ^{2}C−^{2}C bonds cleave via α,β species bound by two C atoms. ^{3}C−^{x}C rupture involves larger $\Delta H^{\ddagger}$ than ^{2}C−^{2}C and ^{2}C−^{1}C because the former requires that more C−H bonds cleave and H* desorb than for the latter two. These endothermic steps are partially compensated by C−metal bond formation, whereas the formation of additional H_2(g) gives larger $\Delta S^{\ddagger}$. C−C rupture transition states for cycloalkanes have less entropy than those for C−C bonds in acyclic alkanes of similar size because C_6 rings decrease the rotational and conformational freedom. $\Delta H^{\ddagger}$ values for all C−C bonds in a given reactant decrease with increasing Ir cluster size because the coordination of exposed metal atoms influences the stabilities of the H* atoms that desorb more than those of the transition states. $\Delta H^{\ddagger}$ for ^{3}C−^{x}C cleavage is more sensitive to cluster size because their transition states displace more H* than those for ^{2}C−^{2}C or ^{2}C−^{1}C bonds. These data and their mechanistic interpretation provide guidance for how surface coordination, reaction temperatures, and H_2 pressures can be used to control ring-opening selectivities toward desirable products while minimizing yield losses. These findings are consistent with trends for the hydrogenolysis of acyclic isoalkanes and seem likely to extend to C−X bond cleavage (where X = O, S, and N atoms) reactions during hydrotreating processes.

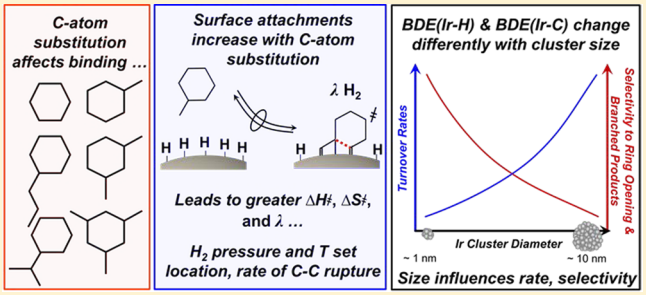

1. INTRODUCTION

Metal clusters catalyze hydrogen-assisted reactions that remove heteroatoms from hydrocarbon streams, saturate arenes, and open cycloalkane rings to give cleaner-burning fuels with higher cetane numbers and lower concentrations of toxic combustion byproducts.[1,2] Endocyclic C−C bond cleavage must be favored over exocyclic cleavage in order to minimize costly yield losses in such processes. The location and rate of C−C bond cleavage in equilibrated arene-cycloalkane-H_2 streams depend on the number and position of alkyl substituents in their C_5 or C_6 rings,[1,3−9] and endocyclic C−C bond cleavage rates are lowest at the most highly substituted C−C bonds (e.g., ^{3}C−^{x}C bonds; superscripts denote the number of C atoms attached) in alkyl cyclohexanes[1,3,4,8,9] and cyclopentanes.[1,6,7] Consequently, ring-opening rates are lower for cycloalkanes with multiple pendant alkyl groups, and such reactants tend to dealkylate or ring-open via C−C rupture at ^{2}C−^{2}C bonds to form highly branched products (e.g., 2,4-dimethylhexane from 1,3-dimethylcyclohexane on Ni, Ru, and Ir).[1] The selectivities toward ^{3}C−^{x}C bond cleavage have been reported to vary with the support identity[3] and with the size[6,7,10] and composition of monometallic[1,6,7,11] and bimetallic catalyst clusters.[12,13]

The fundamental kinetic and thermodynamic underpinnings for these reactivity and selectivity trends, however, remain unclear. The prevalent mechanistic interpretations rely on speculative descriptions of the structure of the reactive intermediates (e.g., α,γ-bound metallacycles for ^{3}C−^{x}C and α,β-tetra-σ adsorbed species for ^{2}C−^{2}C, ^{2}C−^{1}C, and ^{1}C−^{1}C cleavage[6]), without direct evidence of their involvement in the activation of specific C−C bonds or rigorous explanations of why such structures are preferred over other plausible intermediates.

Received: November 21, 2014
Revised: January 7, 2015
Published: January 26, 2015

DOI: 10.1021/jp511688x
J. Phys. Chem. C 2015, 119, 2597−2613

The specificity for cleaving ^{2}C−^{2}C bonds over ^{3}C−^{x}C bonds on metal surfaces contradicts inference from empirical free-energy relations[14] because homolytic C−C dissociation energies (BDE(C−C)) are actually lower for ^{3}C−^{x}C bonds than for ^{2}C−^{2}C or ^{2}C−^{1}C bonds.[15] These differences in BDE(C−C) among C−C bonds with different degrees of substitution indicate that intrinsic activation enthalpies to cleave ^{3}C−^{x}C bonds (H_{act}, i.e., the forward enthalpy barrier for the elementary step that cleaves the C−C bond) should be smaller than for C−C bonds with less-substituted C atoms. Apparent activation enthalpies ($\Delta H^{\ddagger}$, the enthalpy barrier for C−C rupture measured with respect to the appropriate reference state, as described below) for C−C bond cleavage are proportional to BDE(C−C) values (averaged over all C−C bonds) for *n*-alkanes (C_2−C_{10}) under conditions that lead to Ir cluster surfaces saturated with chemisorbed hydrogen (H*).[16,17] $\Delta H^{\ddagger}$ values for ^{3}C−^{x}C bond cleavage in isoalkanes, however, are larger than those for ^{2}C−^{2}C and ^{2}C−^{1}C bonds within a given molecule.[18] These data suggest that BDE(C−C) values alone cannot accurately describe C−C bond reactivity and that a more rigorous analysis is required to account for how H*-saturated surfaces stabilize the relevant C−C bond cleavage transition states in these molecules.

We have previously shown that C−C bond cleavage turnover rates increase with *n*-alkane chain length (C_2−C_{10}).[16] Interpretations based on transition-state theory and statistical mechanics formalisms indicate that these differences in rates reflect $\Delta H^{\ddagger}$ values that are proportional to the average BDE(C−C) values for *n*-alkanes and thus decrease with increasing reactant length. $\Delta S^{\ddagger}$ values concomitantly increase with chain length because the fraction of the total entropy lost upon adsorption (i.e., from diminished translational and rotational freedom) is smaller for larger *n*-alkanes (because of their significant vibrational entropy). These entropy differences are significant because large $\Delta S^{\ddagger}$ values are necessary to overcome the prohibitively high $\Delta H^{\ddagger}$ values (>200 kJ mol^{-1}) for C−C rupture on metals, and because differences between $\Delta S^{\ddagger}$ for different C−C bonds within a given reactant determine, to a significant extent, the location of the C−C bond cleaved.[16] Density functional theory (DFT) treatments have confirmed these mechanistic inferences while also providing quantitative predictions for activation energies and for how the extent of dehydrogenation determines H_{act} values for C−C bond rupture in ethane-derived surface intermediates.[17] Experiments and transition-state theory treatments, based on statistical mechanics, show how and why C−C bond cleavage rates differ between ^{3}C−^{x}C bonds and ^{2}C−^{2}C and ^{2}C−^{1}C bonds within a given isoalkane on Ir, Rh, Ru, and Pt clusters.[18]

Briefly, ^{3}C−^{x}C bond cleavage in acyclic alkanes is mediated by transition states that involve the removal of 4−5 H atoms from the isoalkane reactants and the concomitant formation of one C−M bond (where M represents an exposed metal atom) for each C−H bond ruptured. ^{3}C atoms can form only one C−M bond, thus requiring the additional dehydrogenation of C atoms not involved in the ^{3}C−^{x}C bond cleaved. Bond order conservation then requires that additional H atoms desorb to form additional C−M bonds that bind these neighboring C atoms. This sequence of endothermic steps increases $\Delta H^{\ddagger}$ values and forms gaseous H_2 molecules, leading to $\Delta H^{\ddagger}$ values that are larger for ^{3}C−^{x}C bonds (by 20−70 kJ mol^{-1}) than for ^{2}C−^{2}C and ^{2}C−^{1}C bonds.[18] These larger $\Delta H^{\ddagger}$ values are compensated for, in part, by the significant entropy gains arising from the H_2(g) molecules formed; the formation of 3−4.5 H_2 molecules for each transition state contributes 400−500 J mol^{-1} K^{-1} to these $\Delta S^{\ddagger}$ values. As a result, such activation entropies become large and positive (160−300 J mol^{-1} K^{-1}), in spite of the entropy losses associated with the binding of the reactant alkanes.[16−18]

In this study, we report C−C bond cleavage rates at distinct positions within six differently substituted cyclohexane reactants and interpret them by combining transition state theory and statistical mechanics formalisms to describe their hydrogenolysis turnover rates and selectivities. We show that the extent of dehydrogenation and the site requirements for ^{3}C−^{x}C and ^{2}C−^{2}C bond cleavage transition states for cyclohexanes resemble those for acyclic alkanes, making those previous conclusions generally relevant for hydrogenolysis catalysis. ^{3}C−^{x}C bond cleavage rates in cyclohexanes exhibit larger $\Delta H^{\ddagger}$ and $\Delta S^{\ddagger}$ values and stronger effects of H_2 pressure than less substituted endocyclic C−C bonds. These results indicate that the cleavage of ^{3}C−^{x}C bonds in cyclohexanes involves complexes with fewer H atoms and more C−M bonds than the transition states that mediate the rupture of less substituted C−C bonds. These inferences are consistent with the observed effects of cluster size on hydrogenolysis turnover rates and on the selectivity for cleaving substituted and unsubstituted C−C bonds on Ir-based catalysts. Small Ir clusters bind H* more strongly than large Ir clusters, give lower C−C bond cleavage turnover rates, and show larger differences between $\Delta H^{\ddagger}$ values for ^{3}C−^{x}C and those for ^{2}C−^{2}C bonds. These differences reflect the need to desorb H* from H*-covered surfaces to bind transition states for C−C bond cleavage. Specifically, $\Delta H^{\ddagger}$ values for a given C−C bond are larger on small clusters than on larger clusters because H* desorption steps become more endothermic with decreasing cluster size. This interpretation is also consistent with measured $\Delta H^{\ddagger}$ values for ^{3}C−^{x}C bond cleavage that are more sensitive to the H*-binding strength (and thus on the size of Ir clusters) than for ^{2}C−^{2}C bond cleavage because the transition states that cleave ^{3}C−^{x}C bonds require the desorption of a larger number of H* atoms than those involved in the cleavage of ^{2}C−^{2}C bonds. These findings also show that differences in the site requirements (e.g., the number of unoccupied sites required to bind the transition state) between ^{3}C−^{x}C and ^{2}C−^{2}C bond rupture transition states lead to different $\Delta H^{\ddagger}$ and $\Delta S^{\ddagger}$ values for the ring opening of alkyl cyclohexane rings at specific locations. These differences in site requirements also account for how rates and product selectivities depend on H_2 pressure on the H*-covered surfaces that prevail during catalytic hydrogenolysis. As a result, we report predictive guiding rules and strategies for controlling the degree of branching in the products formed in ring-opening reactions via C−C rupture (and plausibly also for C−S, C−O, and C−N cleavage) through rigorous mechanistic interpretations of the measured effects of temperature, H_2 pressure, and the size of the catalytic metal clusters.

2. EXPERIMENTAL METHODS

2.1. Synthesis of Supported Ir Catalysts. Silica (Davisil 646, 300 m^2 g^{-1}) was used as the catalyst support and was treated in flowing dry air (Praxair, 99.99%, 5.0 cm^3 g^{-1} s^{-1}) by heating to 823 K at 0.03 K s^{-1} and holding for 5 h. Ir was deposited onto SiO_2 via aqueous solutions (deionized water, 17.9 MΩ resistivity) of triethanolamine (TEA, Sigma-Aldrich, 97%) and H_2IrCl_6 (Strem Chemicals, 99%) (10:1−20:1 mol/

DOI: 10.1021/jp511688x
J. Phys. Chem. C 2015, 119, 2597−2613

Table 1. Catalyst Synthesis Conditions and Characterization

			temperature (K)		fractional dispersion				
sample	TEA/M[a]	metal content (wt %)	oxidative treatment[b]	reductive treatment[c]	H_2[d]	O_2[e]	CO[f]	$\langle d_{chem}\rangle$ (nm)[g]	$\langle d_{TEM}\rangle$ (nm)[h]
0.7 nm Ir	20	1.0	573 (1 h)	873 (3 h)	1.4	1.7	1.5	0.7	0.8
3 nm Ir	10	2.0	673 (2 h)	723 (3 h)	0.36	0.35		2.7	6.2
7 nm Ir	10	3.0	1123 (12 h)	1173 (8 h)	0.13	0.15	0.13	7.1	14

[a]Ratio of triethanol amine to metal precursor in the aqueous solution used for SiO_2 impregnation. [b]21 kPa O_2 (dry air). [c]50 kPa H_2 (balance He). [d]H_2 chemisorption (irreversible uptake at 300 K), assuming $H/M_s = 1$. [e]O_2 chemisorption (irreversible uptake at 300 K), assuming $O/M_s = 1$. [f]CO chemisorption (irreversible uptake at 300 K), assuming $CO/M_s = 1$. [g]Mean particle diameters, $\langle d_{chem}\rangle$, calculated using the average fractional dispersion from all titrants used and assuming hemispherical clusters with densities equal to those of bulk metal (section 2.2). [h]Surface-averaged mean particle diameter from TEM analysis (section 2.2).

mol).[16] The Ir−SiO_2 materials (1.0−3.0 wt % Ir) were prepared by adding these aqueous solutions dropwise onto treated SiO_2 until the point of incipient wetness. The impregnated samples were then heated to 393 K at 0.017 K s^{-1} in flowing dry air and held for 12 h, after which the powders were heated to 573 K at 0.017 K s^{-1} in flowing dry air and held for 1 h with the intent to cause condensation reactions between the TEA complexes and surface silanol groups.[19] These samples were then heated to 673 K at 0.033 K s^{-1} in flowing 50% H_2/He (Praxair, 99.999%, 1.0 cm^3 g^{-1} s^{-1}) and held for 3 h to form supported metallic Ir clusters. The materials were then cooled to ambient temperature and passivated in flowing 0.5% O_2/He (Praxair, 99.99%, 1.0 cm^3 g^{-1} s^{-1}) for 6 h before exposure to ambient air. The sizes of the Ir clusters were varied by subsequent oxidative and reductive treatments as described in Table 1.

2.2. Catalyst Characterization. The number of exposed Ir surface atoms (Ir_s) in each catalyst was determined by averaging the volumetric uptakes of H_2, O_2, and CO at 298 K,[16,20] and the Ir content of each sample was measured using inductively coupled plasma optical emission spectroscopy (ICP-OES, Galbraith). Mean Ir cluster diameters ($\langle d_{chem}\rangle$) were estimated from the number of titrants irreversibly adsorbed and by assuming hemispherical crystallites and adsorption stoichiometries of H/Ir_s, O/Ir_s, and CO/Ir_s of unity. The $\langle d_{chem}\rangle$ values from H_2, O_2, and CO chemisorption are shown in Table 1. The mean values of $\langle d_{chem}\rangle$, calculated from the averaged values from the three titrants, are 0.7, 2.7, and 7.1 nm for the 1.0, 2.0, and 3.0 wt % Ir catalysts, respectively.

Cluster size distributions were measured from transmission electron microscopy (TEM) images for each sample in bright-field mode (Philips, CM200F) using samples dispersed onto Cu grids coated with lacey carbon. The surface-averaged cluster diameter ($\langle d_{TEM}\rangle$) is the most appropriate method for weighting cluster sizes because it reflects the number of surface atoms available for adsorption and catalysis. Values of ($\langle d_{TEM}\rangle$) were calculated using

$$\langle d_{TEM}\rangle = \frac{\sum n_i d_i^3}{\sum n_i d_i^2} \quad (1)$$

where n_i is the number of clusters with a diameter d_i from >1000 clusters. The values of $\langle d_{TEM}\rangle$ and $\langle d_{chem}\rangle$ are similar for the 0.7 nm sample (Table 1), but the samples with larger average Ir cluster sizes (3 and 7 nm) seem to contain a bimodal distribution that includes a significant number of small clusters that were not observed by TEM at the level of magnification used. Consequently, $\langle d_{TEM}\rangle$ values for these samples are larger than $\langle d_{chem}\rangle$ (Table 1). Values of $\langle d_{chem}\rangle$ directly reflect the total number of exposed metal atoms and, in these cases, are the most accurate measure of the mean cluster size because TEM estimates these numbers indirectly. Consequently, we refer to metal clusters using their chemisorption-derived sizes ($\langle d_{chem}\rangle$ denoted as 0.7, 3, and 7 nm). Representative TEM images and cluster size histograms are included in the Supporting Information (Figures S1−S3).

2.3. Hydrogenolysis Turnover Rates and C−C Cleavage Selectivities. Hydrogenolysis rates were measured using a stainless steel tubular reactor (3/8 in. o.d.) with plug-flow hydrodynamics, which is contained within a three-zone resistively heated furnace (Applied Test Systems). The bed temperature was measured with a type-K thermocouple held within a 1/16 in. stainless steel sheath mounted axially within the catalyst bed, and the temperature of each zone was regulated using an electronic PID controller (Watlow, EZ-Zone). Catalysts were mixed with additional SiO_2 (Cab-O-Sil HS-5, washed with deionized water and treated in flowing dry air at 793 K for 5 h) to avoid axial and radial temperature gradients. The pressure was controlled using a backpressure regulator (Mity-Mite, model S91XW). The catalyst was treated in flowing H_2 (Praxair, 99.999%, 50 cm^3 g^{-1} s^{-1}) at ambient pressure by heating to 673 K at 5 K min^{-1} and holding for 2 h before rate measurements were made. The molar flow rates and composition of the reactant stream were set using electronic mass flow controllers (Parker, model 201). All liquid hydrocarbons were obtained from Sigma-Aldrich (cyclohexane, anhydrous, 99.5%; toluene, anhydrous, >99.8%; 1,3-dimethylcyclohexane, 99%; 1,3,5-trimethylbenzene; 98%; *n*-propylbenzene, >99%; and isopropylbenzene, >98%) and were introduced using a high-pressure syringe pump (Isco, 500D). H_2 (Praxair, 99.999%) flow rates were set by electronic mass flow controllers (Parker, model 201). Transfer lines before and after the reactor were maintained at 423 K to prevent condensation.

The concentrations of reactants and products were measured with gas chromatography (Agilent GC, 5890) using a methyl silicone capillary column (HP-1, 50 m × 0.32 mm × 1.05 μm) and a flame ionization detector. The retention time for each component was determined using isoparaffin (Sigma-Aldrich, isoparaffins mix, 44586-U) and naphthene (Sigma-Aldrich, naphthenes mix, 44588) standard mixtures, and molecular speciation was confirmed by mass spectrometry (Agilent, 5975C). Turnover rates were measured under differential conditions (<10% reactant conversion) to ensure that products were formed in primary reactions and reactant depletion did not affect measured rates. Turnover rates are reported as moles of carbon converted per second per mole of Ir_s ((mol C) (mol Ir_s s)$^{-1}$).

DOI: 10.1021/jp511688x
J. Phys. Chem. C 2015, 119, 2597−2613

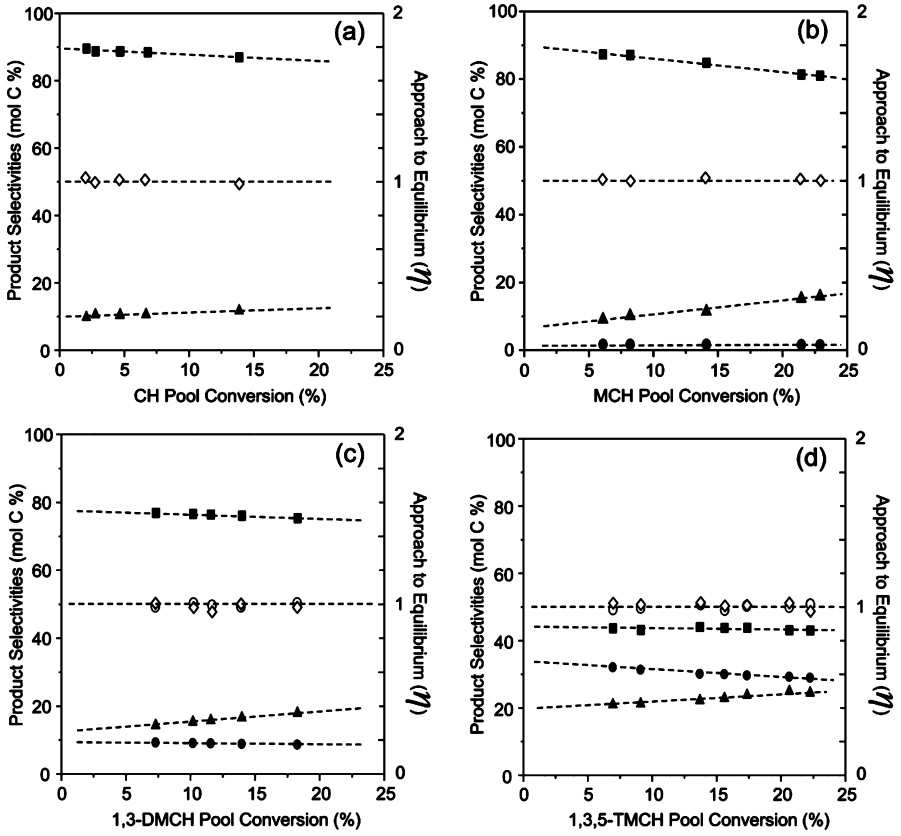

Figure 1. Hydrogenolysis product selectivities and approach to equilibrium factors (η, eqs 4 and 5) for (a) cyclohexane (CH), (b) methylcyclohexane (MCH), (c) 1,3-dimethylcyclohexane (1,3-DMCH), and (d) 1,3,5-trimethylcyclohexane (1,3,5-TMCH) reactants on 0.7 nm Ir clusters for 20 kPa cycloalkanes, 3.4 MPa H_2, and 593 K. These plots show selectivities toward products from ring opening ($^3C-^2C$ and $^2C-^2C$ bond cleavage) (■), dealkylation ($^3C-^1C$ bond cleavage) (●), and multiple hydrogenolysis (▲) reaction pathways as a function of the conversion of the reactant pool, which consists of equilibrated mixtures of cycloalkanes, arenes, and H_2 as shown by η values for dehydrogenation (◊) and isomerization (○) near unity. Dashed lines represent linear fits.

3. RESULTS AND DISCUSSION

3.1. C−C Bond Cleavage Locations, Elementary Steps, and Rate Equations. Figure 1 shows hydrogenolysis product selectivities for cyclohexane (CH, Figure 1a), methylcyclohexane (MCH, Figure 1b), 1,3-dimethylcyclohexane (1,3-DMCH, Figure 1c), and 1,3,5-trimethylcyclohexane (1,3,5-TMCH, Figure 1d) reactants as a function of reactant conversion on 0.7 nm Ir clusters (20 kPa hydrocarbon, 3.4 MPa H_2, 593 K). C−H bond cleavage and formation steps precede C−C bond cleavage in acyclic[16−18,21−24] and cyclic[6,8,25−27] alkanes, including CH, MCH, 1,3-DMCH, and 1,3,5-TMCH. The dehydrogenation of cyclohexanes forms arenes

$$C_nH_{2n} \rightleftarrows C_nH_{2n-6} + 3H_2 \quad (2)$$

and parallel isomerization reactions form mixtures of the cis and trans isomers of reactants with multiple substituents, such as 1,3-DMCH and 1,3,5-TMCH:

$$cis\text{-}C_nH_{2n} \rightleftarrows trans\text{-}C_nH_{2n} \quad (3)$$

The approach to equilibrium factors for dehydrogenation (η_H) and isomerization (η_I) of cyclohexane reactants is given by

$$\eta_H = \frac{(C_nH_{2n-6})(H_2)^3}{(C_nH_{2n})K_H} \quad (4)$$

$$\eta_I = \frac{(C_nH_{2n,trans})}{(C_nH_{2n,cis})K_I} \quad (5)$$

where the parentheses indicate the pressure of each molecule in units of bars and K_H and K_I are the equilibrium constants for dehydrogenation and isomerization, respectively. Figure 1 shows that η_H and η_I values are near unity and independent of space velocity and reactant conversion for all cyclohexanes, indicating that cycloalkanes and their unsaturated and isomeric products can be treated as an equilibrated reactant pool. Conversion, therefore, can be rigorously defined based on the number of molecules that are removed from this pool via hydrogenolysis reactions. The equilibrated nature of dehydrogenation reactions requires that all intervening steps (H_2 and cycloalkane adsorption−desorption and C−H bond formation-cleavage) occur much faster than C−C bond scission and are therefore also quasi-equilibrated. These data (Figure 1) show that kinetically relevant C−C bond cleavage occurs in a quasi-equilibrated pool of adsorbed reactants, consisting of the cyclohexane and all intervening dehydrogenated and isomerized cyclic species.

The initial hydrogenolysis event cleaves either an endocyclic C−C bond (i.e., $^3C-^2C$, $^2C-^2C$) to form a ring-opening (RO) product (with the same number of C atoms as the reactant) or an exocyclic C−C bond (i.e., $^3C-^1C$) to form a dealkylation (DA) products (two fragments, each with fewer C atoms than the reactant). RO and DA selectivities decreased with

DOI: 10.1021/jp511688x
J. Phys. Chem. C 2015, 119, 2597−2613

increasing pool conversion for all cyclohexanes (Figure 1) because secondary C−C bond cleavage of primary products leads to multiple hydrogenolysis (MH) events that form molecules with fewer C atoms than the reactants. Selectivities extrapolated to zero conversion (Figure 1) reflect those reactions that occur during a single surface sojourn with minimal contributions from secondary reactions. These primary selectivities are higher for ring opening than for dealkylation reactions, indicating that endocyclic C−C bond cleavage is more facile than exocyclic C−C bond cleavage for all methyl-substituted cyclohexanes (Figure 1b−d). Primary ring-opening selectivities decreased as the number of methyl ring substituents increased (90% RO selectivity for MCH, Figure 1b; 44% for 1,3,5-TMCH, Figure 1d), whereas DA and MH selectivities concurrently increased. These DA selectivities (2% for MCH, Figure 1d; 35% for 1,3,5-TMCH, Figure 1d) increased more than proportionally with the number of methyl substituents, indicating that selectivities do not simply reflect the number of endocyclic and exocyclic C−C bonds but also the degree of substitution at the endocyclic C−C bonds, which increases as more methyl groups are present on the ring. Such trends have been reported previously[1,3,4,8] and show that apparent rate constants for C−C rupture decrease as the substitution of the C atoms involved increases (e.g., rate constants for $^{3}C-^{1}C$ rupture are less than for $^{2}C-^{2}C$ rupture).

Extrapolated MH selectivities are nonzero (Figure 1), showing that multiple C−C bonds can cleave in one surface sojourn to cluster surfaces, although these reactions may also occur as primary products diffuse through the porous catalyst before entering the moving fluid phase. Initial MH selectivities increased with an increasing number of ring substituents (from 8% for MCH to 20% for 1,3,5-TMCH; Figure 1b,d); cyclohexane rings with larger numbers of substituents have a greater tendency to react via MH pathways, which lead to a larger number of light products. The high selectivity of 1,3,5-TMCH conversion to MH products shows that the rate constants for C−C cleavage within dealkylation (1,3-DMCH) and ring-opening (2,4-dimethylheptane) products, which contain $^{2}C-^{2}C$ and $^{2}C-^{1}C$ bonds, are higher than $^{3}C-^{x}C$ rupture rate constants in the 1,3,5-TMCH reactant. The mechanisms by which substitution affects hydrogenolysis rates are discussed in detail below.

The underlying mechanistic bases for the low C−C rupture rates at substituted endocyclic positions and for the concomitant decrease in RO selectivities with the number of ring substituents remain uncertain in the literature.[1,3,4,8,25,28] On the basis of the different site requirements and extents of dehydrogenation for transition states that rupture $^{3}C-^{x}C$ bonds and those that cleave $^{2}C-^{2}C$ bonds in acyclic alkanes,[18] it seems reasonable that similar mechanisms would also account for the differences in rupture rates at substituted and unsubstituted positions in cycloalkanes. To test this hypothesis, we have considered the implications of the effects of cycloalkane structure and concentration and temperature on rupture rates to identify plausible intermediates and transition states and their structure, surface coordination, and extent of dehydrogenation.

Figure 2 shows hydrogenolysis turnover rates as a function of cycloalkane pressure at H_2/C_nH_{2n} ratios of 8−100 for MCH and 1,3-DMCH (Figure 2a) and at higher H_2/C_nH_{2n} ratios (25−500) for CH, MCH, and 1,3-DMCH (Figure 2b) on 0.7 nm Ir clusters. C−C bond cleavage rates do not depend on the hydrocarbon pressure ($r \approx (C_nH_{2n})^0$, Figure 2a) for H_2/C_nH_{2n} ratios below 100. Hydrogenolysis rates, however, are proportional to hydrocarbon pressures for H_2/C_nH_{2n} ratios above 200 (Figure 2b, where (C_nH_{2n}) <25 kPa). Figure 3 shows that CH, MCH, 1,3-DMCH, *n*-propylcyclohexane (*n*-PCH), and isopropylcyclohexane (i-PCH) hydrogenolysis rates all depend sensitively and similarly on H_2 pressure. Specifically, rates increased with increasing H_2 pressure for H_2/C_nH_{2n} ratios below 40, reached a maximum at 60−65 H_2/C_nH_{2n}, and then decreased at higher H_2 pressures with a functional dependence described by $r \approx (H_2)^{-\lambda}$ (where $\lambda > 0$). These trends are similar to those previously reported for the hydrogenolysis of ethane,[17,21,23,24,29,30] *n*-alkanes,[16,29−31] and isoalkanes.[18,30] These λ values differ among cyclohexane reactants ($1.5 < \lambda < 3.0$, Table 2; uncertainties of ±0.2−0.5) but become nearly constant at the highest H_2/C_nH_{2n} ratios (250−275), indicating that λ depends on the number and structure of the alkyl substituents in the cyclohexane ring (methyl, isopropyl, and *n*-propyl). The λ values for substituted cyclohexanes (λ = (2.4−3.0) ± 0.5, Table 2), which contain ^{3}C atoms, are larger than for cyclohexane (λ = 1.8 ± 0.4), which contains only $^{2}C-^{2}C$ bonds. Such differences are reminiscent of λ values for $^{3}C-^{x}C$ bonds in acyclic isoalkanes (λ = (3.5−4.5) ± 0.2)[18] that are also larger than for $^{2}C-^{2}C$ and $^{2}C-^{1}C$ bonds in acyclic alkanes (λ = 3.0 ± 0.2).[16]

The observed effects of H_2 and cycloalkane pressures on C−C bond cleavage rates are consistent with the sequence of elementary steps shown in Scheme 1. These steps include

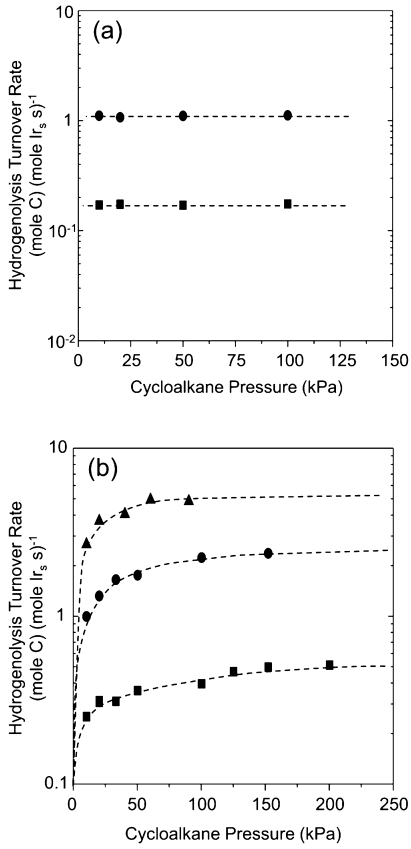

Figure 2. Hydrogenolysis turnover rates as a function of cycloalkane feed pressure at (a) low H_2 pressures for methylcyclohexane (●, 0.8 MPa H_2) and 1,3-dimethylcyclohexane (■, 1.0 MPa H_2) and (b) high H_2 pressures for cyclohexane (▲, 1.8 MPa H_2), methylcyclohexane (●, 5.0 MPa H_2), and 1,3-dimethylcyclohexane (■, 5.0 MPa H_2) on 0.7 nm Ir clusters at 593 K. Dashed curves indicate trends.

DOI: 10.1021/jp511688x
J. Phys. Chem. C 2015, 119, 2597−2613

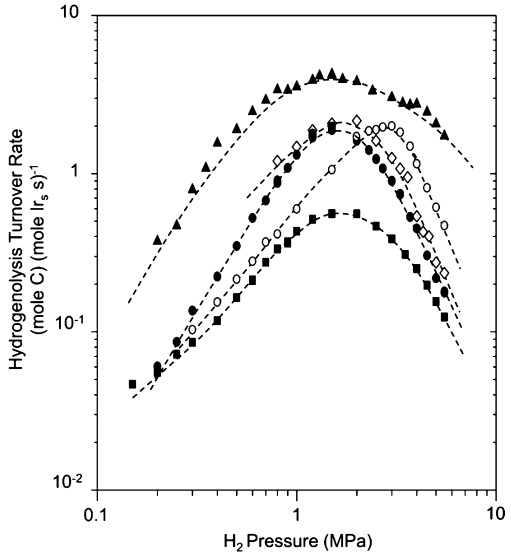

Figure 3. Hydrogenolysis turnover rates as a function of H_2 pressure at 20 kPa cycloalkane for cyclohexane (▲), methylcyclohexane (●), *n*-propylcyclohexane (◊), isopropylcyclohexane (○), and 1,3-dimethylcyclohexane (■) reactants on 0.7 nm Ir clusters at 593 K. Dashed curves represent trends.

Table 2. Values of λ for Cycloalkane Hydrogenolysis on Hydrogen-Covered Surfaces of 0.7 nm Ir Clusters Supported on Silica[a]

cycloalkane	λ
cyclohexane	1.8 ± 0.4
methylcyclohexane	3.0 ± 0.2
1,3-dimethylcyclohexane	2.4 ± 0.5
n-propylcyclohexane	2.5 ± 0.5
isopropylcyclohexane	2.8 ± 0.5

[a]The value of λ for each cycloalkane was determined from the dependence of hydrogenolysis rates on H_2 pressure (Figure 3) at high (>70) H_2/C_nH_{2n} ratios and 593 K.

quasi-equilibrated H_2 dissociation (step 1.1) and adsorption (step 1.2) and the dehydrogenation (steps 1.3−1.5) of cyclic alkanes (C_nH_{2n}); these steps lead to the formation of an equilibrated pool of unsaturated intermediates containing y fewer H atoms than the C_nH_{2n} reactants (i.e., C_nH_{2n-y}, where $1 \le y \le 2n$). C−C bonds can cleave (step 1.6) in all adsorbed intermediates ($C_nH_{2n-y}(\gamma^*)$, where γ is the number of sites that bind the intermediate), but their relative C−C bond cleavage rates depend sensitively on the number and location of the H atoms removed and of the surface attachments formed at the transition state.

All hydrogenation−dehydrogenation reactions of the products are also in thermodynamic equilibrium. For example, the dealkylation of MCH forms equilibrated mixtures of cyclohexane, benzene (as well as all intervening unsaturated intermediates such as cyclohexene and cyclohexadiene, whose equilibrium concentrations lie below the detection limits of our chromatographic protocols), and H_2, whereas ring opening forms equilibrated mixtures of acyclic alkanes and alkenes with H_2. We conclude from the equilibrium concentrations of these detectable species (e.g., cyclohexane, benzene, and H_2) that hydrogenation and desorption processes (step 1.7) also attain equilibrium.

Scheme 1. Proposed Intermediate Steps for Cycloalkane Hydrogenolysis on Metal Cluster Surfaces[a]

$$H_2 + 2^* \underset{k_{-H2}}{\overset{k_{H2}}{\rightleftharpoons}} 2\,H\text{-}^* \quad (1.1)$$

$$C_nH_{2n} + ^* \underset{k_{-A}}{\overset{k_A}{\rightleftharpoons}} C_nH_{2n+2}\text{-}^* \quad (1.2)$$

$$C_nH_{2n}\text{-}^* + ^* \underset{k_{-CH,1}}{\overset{k_{CH,1}}{\rightleftharpoons}} C_nH_{2n-1}\text{-}^* + H\text{-}^* \quad (1.3)$$

$$C_nH_{2n-1}\text{-}^* + 2^* \underset{k_{-CH,2}}{\overset{k_{CH,2}}{\rightleftharpoons}} C_nH_{2n-2}\text{-}2^* + H\text{-}^* \quad (1.4)$$

$$\rightrightarrows$$

$$C_nH_{2n-(y-1)}\text{-}\gamma^* + ^* \underset{k_{-CH,y}}{\overset{k_{CH,y}}{\rightleftharpoons}} C_nH_{2n-y}\text{-}\gamma^* + H\text{-}^* \quad (1.5)$$

$$C_nH_{2n-y}\text{-}\gamma^* \xrightarrow{k_{CC,y}} C_aH_{a'}\text{-}a''^* + C_bH_{b'}\text{-}b''^* \quad (1.6)$$

$$C_aH_{a'}\text{-}a''^* + xH\text{-}^* \underset{k_{-Ca}}{\overset{k_{Ca}}{\rightleftharpoons}} C_aH_{2a+2} + (a''+x)^* \quad (1.7)$$

[a]* denotes an unoccupied surface site; $X-n^*$ denotes an intermediate (X) bound to n sites; ⇄ with ○ denotes a quasi-equilibrated step; k_x and K_x represent kinetic and equilibrium constants, respectively, for each elementary step; y is the number of H atoms removed from the cycloalkane to form the reactive intermediate leading to the kinetically relevant transition state; and γ is the number of sites required to bind the transition state.

Cycloalkane hydrogenolysis occurs at rates (Figures 2 and 3) given by the combined rates of cleavage of all endocyclic and exocyclic C−C bonds in the quasi-equilibrated reactant pool. C−C bonds cleave in intermediates with y missing H atoms and bound at γ binding sites ($C_nH_{2n-y}(\gamma^*)$) at rates equal to the product of their respective reaction rate constants for cleavage at each C−C bond ($k_{CC,y}$) and the number of intermediates involved ($[C_nH_{2n-y}(\gamma^*)]$):

$$r_y = k_{CC,y}[C_nH_{2n-y}(\gamma^*)] \quad (6)$$

The pseudo-steady-state hypothesis (PSSH) for each $[C_nH_{2n-y}(\gamma^*)]$ intermediate leads to the following rate equation for hydrogenolysis steps proceeding through that intermediate:

$$r_y = k_{app,CC,y}(C_nH_{2n})(H_2)^{-y/2}\frac{[*]^\gamma}{[L]^{\gamma-1}} \quad (7)$$

In eq 7, $k_{app,CC,y}$ is the apparent rate constant for cleaving a given C−C bond in $C_nH_{2n-y}(\gamma^*)$, which depends on the combined free-energy change involved in forming $C_nH_{2n-y}(\gamma^*)$ from the cycloalkane reactant (Scheme 1, steps 1.1−1.5) and then the C−C rupture transition states (Scheme 1, step 1.6). The [*] term represents the number of unoccupied sites on cluster surfaces, and [L] is the total number of active sites, taken here as the number of exposed Ir surface atoms determined from chemisorption uptake and used to express the reactivity as a turnover rate. This rate expression depends on $[*]^\gamma$ because transition states for C−C bond cleavage bind to γ ($\gamma \ge 1$) vicinal sites, as inferred from theoretical[8,22,26,27,32] and experimental[16−18,21] studies of the hydrogenolysis of acyclic and cyclic alkanes. The full form of the rate equation is

$$\frac{r_y}{[L]} = k_{CC,y}\frac{(\prod_{i=1}^{y} K_{CH,i})K_A(C_nH_{2n})(H_2)^{-y/2}}{(1 + (C_nH_{2n})[*]^{\gamma-1}\sum_{z=1}^{2n}(\prod_{i=1}^{z} K_{CH,i}K_A(H_2)^{-z/2}) + (K_{H_2}(H_2))^{1/2})^\gamma} \quad (8)$$

DOI: 10.1021/jp511688x
J. Phys. Chem. C 2015, 119, 2597−2613

Here, K_{H_2} and K_A are the equilibrium constants for H_2 and C_nH_{2n} adsorption, respectively, and $\Pi_{i=1}^{x}K_{CH,i}$ is the product of all equilibrium constants for the C−H cleavage steps that dehydrogenate C_nH_{2n} to form an intermediate with C_nH_{2n-x} stoichiometry. The three terms in the denominator of eq 8 represent the relative number of sites that are unoccupied (the 1 term), occupied by species within a cycloalkyl "zoo"[33] ($((C_nH_{2n})[*]^{\gamma-1}\Sigma_{z=1}^{2n}(\Pi_{i=1}^{z}K_{CH,i}K_A(H_2)^{-z/2}))$, and occupied by H* ($(K_{H_2}(H_2))^{1/2}$). Equation 8 has a complex form that can be rigorously interpreted only at its asymptotic limits, when either the equilibrated pool of cyclic hydrocarbons, H* atoms, or unoccupied sites represent the only most abundant surface intermediates (MASI).[16]

At low H_2/C_nH_{2n} ratios, Ir surfaces become saturated with the equilibrated pool of cycloalkane-derived intermediates $C_nH_{2n-z}(\gamma^*)$, where z ranges between values of 0 and $2n$, and the concentration of species with each z value depends on the prevalent H_2 pressure and on the equilibrium constants for cycloalkane dehydrogenation to C_nH_{2n-z} and for the adsorption of C_nH_{2n-z} onto Ir cluster surfaces. On hydrocarbon-saturated surfaces, turnover rates increase with H_2 pressure (Figure 3) and are independent of C_nH_{2n} pressure (Figure 2a). These data (Figures 2a and 3) are consistent with the simplified form of eq 8 when C_nH_{2n-z} becomes the MASI at H_2/C_nH_{2n} ratios below 100:

$$\frac{r_y}{[L]} \approx (H_2)^{-(y-\langle z\rangle)/2} \tag{9}$$

Here, $\langle z\rangle$ is the mean number of H atoms that are lost from reactants in forming the cycloalkane-derived surface intermediates, which is determined from the functional dependence of the summed concentrations of all $C_nH_{2n-z}(\gamma^*)$ species ($\Sigma_{z=1}^{2n}(\Pi_{i=1}^{z}K_{CH,i}K_A(H_2)^{-z/2})$, eq 8) on the prevalent H_2 pressure. Hydrogenolysis rates that increase with H_2 pressure on surfaces saturated with C_nH_{2n-z} species (Figure 3, 0.15−2 MPa H_2) indicate that the components of this pool that actually cleave C−C bonds in cyclic reactants are more hydrogenated, on average, than the entire pool of surface intermediates (i.e., $y < \langle z\rangle$).

At high H_2/C_nH_{2n} ratios (Figure 3), cluster surfaces become saturated with H* and turnover rates depend on both C_nH_{2n} and H_2 pressures, which determine the surface concentration of the $C_nH_{2n-y}(\gamma^*)$ species that cleave the C−C bonds. In this case, eq 8 simplifies to

$$\frac{r_y}{[L]} = k_{CC,y}\frac{(\prod_{i=1}^{y}K_{CH,i})K_A(C_nH_{2n})}{K_{H_2}(H_2)^{y+\gamma/2}} \tag{10}$$

High H_2/C_nH_{2n} ratios lead to saturation coverages of H*, which require that

$$(K_{H_2}(H_2))^{1/2} \gg (C_nH_{2n})[*]^{\gamma-1}\sum_{z=1}^{2n}\left(\prod_{i=1}^{z}K_{CH,i}K_A(H_2)^{-z/2}\right) \tag{11}$$

In eq 11, the left and right sides represent the number of sites occupied by H* ([H*]) and by the cycloalkyl "zoo",[33] respectively.[16] Equation 10 accurately describes the measured effects of C_nH_{2n} and H_2 pressures on hydrogenolysis rates at H_2/C_nH_{2n} ratios above 200, which appear to lead to H*-saturated surfaces. Under these conditions rates become proportional to the cycloalkane pressure (Figure 2b) and decrease with increasing H_2 pressure (Figure 3). Measurements of the effects of H_2 pressure on hydrogenolysis turnover rates for H*-covered surfaces ($r \approx (H_2)^{-\lambda}$, eq 10) give values of λ that can be used, in turn, to estimate y and γ using the relationship $\lambda = (\gamma + y)/2$. These H_2 pressure effects and the resulting values of y and γ, which are individually estimated using bond order conservation arguments, provide essential insights into the differences between the extent of dehydrogenation and binding modes, respectively, of transition states that rupture $^3C-^xC$ bonds and those that cleave C−C bonds containing unsubstituted C atoms in cyclohexanes.

3.2. Effects of Alkyl Substitution on Endocyclic C−C Bond Cleavage Rates in Cycloalkanes. Vibrational spectra for chemisorbed hydrocarbons[34−37] and DFT calculations[26,27,38,39] have shown that at temperatures required for ring opening (>500 K) unsaturated hydrocarbons bind to metal surfaces by forming C−M bonds to all C atoms that are not sp^3 hybridized. These chemisorbed species resemble surface intermediates that form via quasi-equilibrated cycloalkane dehydrogenation and subsequently undergo C−C bond cleavage. C−M bond dissociation energies (BDE(C−M))[35,40−42] and the reported values of BDE(C−C)[43] and BDE(C−H)[43] indicate that adsorbed hydrocarbons become more enthalpically stable (by ≥100 kJ mol^{-1}) when they form C−M bonds, instead of C═C bonds or radical species, at each C atom upon loss of an H atom. These C−M bonds require that H* atoms desorb from H*-saturated surfaces as $H_2(g)$ ($\Delta H_{des,H^*}$ = 17 kJ mol^{-1} at H^*/Ir_s = 1 on Ir(111) at 593 K[17]). Thus, one M−H bond must break for each C atom that undergoes dehydrogenation because differences between the relevant bond energies lead to a significant preference for the formation of C−M bonds over C═C bonds upon dehydrogenation.

Table 3 shows λ values for all distinct C−C bonds in cyclohexanes, which include endocyclic and exocyclic C−C bonds at substituted ($^3C-^xC$) and unsubstituted ($^2C-^2C$ and $^2C-^1C$) positions. These λ values are larger (by 0.5−1.1) for $^3C-^xC$ bonds (λ = 1.6−4.1) than for $^2C-^2C$ and $^2C-^1C$ bonds (λ = 1.5−2.9) for each cycloalkane, indicating that the combined number of H atoms removed from the cycloalkane (y, eqs 8 and 10) and desorbed from the surface to bind C atoms (γ, eqs 8 and 10) depends on the degree of substitution of C atoms at the cleaved C−C bond, irrespective of its endocyclic or exocyclic location. These results are similar to the trends in λ values found for $^3C-^xC$ and $^2C-^2C$ or $^2C-^1C$ bonds in n-alkanes and isoalkanes[18] and are consistent with previously reported effects of H_2 pressure on MCH ring-opening rates and selectivities.[8] The mechanistic significance of these λ values for cyclohexanes is readily shown to reflect the sum of the number of C−H (y) and M−H (γ) bonds cleaved to form the relevant transition state (eq 10) because dehydrogenation and adsorption are fully equilibrated ($\eta_H \rightarrow 1$, Figure 1) under all reaction conditions.

Stoichiometry, bond order conservation arguments,[18] and theoretical treatments[17] provide the necessary guidance for estimating the individual values of y and γ because the kinetic effects of H_2 pressure reflect only their sum (eq 10). A combined experimental and theoretical study showed that the $^1C-^1C$ bond in ethane cleaves on H*-covered Ir surfaces via a tetra-σ-bound α,β-coordinated intermediate (*CHCH*) with y and γ values of 4 and 2, respectively (i.e., λ = 3).[17] The value of λ for cleaving $^2C-^2C$ and $^2C-^1C$ bonds in n-alkanes (C_3-C_{10})

DOI: 10.1021/jp511688x
J. Phys. Chem. C 2015, 119, 2597−2613

Table 3. λ, $\Delta H^{\ddagger}$, $\Delta S^{\ddagger}$, and $\Delta G^{\ddagger}$ Values for Cleaving Designated C−C Bonds in Cycloalkanes on Hydrogen-Covered Surfaces of 0.7 nm Ir Clusters Supported on Silica[a]

Alkane	C-C Bond	λ	$\Delta H^{\ddagger}$ (kJ mol^{-1})	$\Delta S^{\ddagger}$ (J mol^{-1} K^{-1})	$\Delta G^{\ddagger}$ (kJ mol^{-1})
Cyclohexane		1.8	-	-	-
Methylcyclohexane		2.9	204	173	102
		2.9	211	192	97
		4.0	273	302	94
		4.1	240	253	90
n-Propylcyclohexane		2.6	180	143	96
		2.7	188	159	94
		3.6	229	239	88
		3.5	236	243	92
		2.9	255	301	77
		2.9	215	205	93
1,3-Dimethylcyclohexane		1.5	-	-	-
		1.9	-	-	-
		2.4	-	-	-
		2.6	-	-	-

[a]Values of $\Delta G^{\ddagger}$ were determined from $\Delta G^{\ddagger} = \Delta H^{\ddagger} - T\Delta S^{\ddagger}$ evaluated at 593 K.

is also equal to 3,[16] suggesting that the transition states for the hydrogenolysis of *n*-alkanes also resemble tetra-σ-bound α,β-coordinated surface intermediates. ^{3}C atoms, however, can lose only their single H atom and therefore can form only one C−M bond. Consequently, y values larger than 3 for ^{3}C−^{2}C bonds (and larger than 4 for ^{3}C−^{1}C bonds) require that H atoms are removed from three or more C atoms in the alkane reactant. Each additional C atom that loses one or more H atom must then form C−M bonds and bind at either an on-top, bridge, or three-fold site to preserve its sp^3 hybridization (i.e., tetrahedral configuration),[36,38,44−46] a process that requires the removal of the required number of H* atoms from H*-covered surfaces. These arguments, taken together with the measured λ values for ^{3}C−^{x}C bond cleavage (Table 3), indicate that these kinetically relevant transition states require a larger number of binding sites and bind more C atoms to the surface ($\gamma \geq 3$) than do the transition states involved in ^{2}C−^{2}C bond cleavage ($\gamma = 2$).

Figure 4 shows the effects of H_2 pressure on the total rates of endocyclic C−C bond cleavage (e.g., ^{2}C−^{2}C and ^{3}C−^{2}C

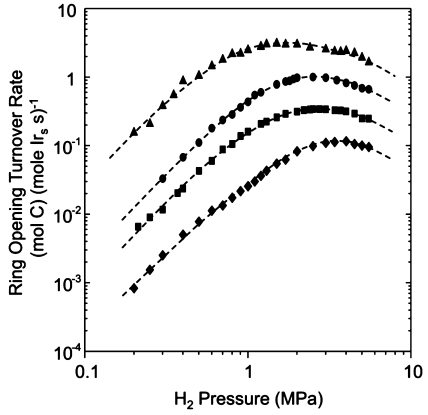

Figure 4. Ring-opening (combined rates of ^{3}C−^{2}C and ^{2}C−^{2}C cleavage at endocyclic positions) turnover rates as a function of H_2 pressure for 20 kPa cycloalkanes for cyclohexane (▲), methylcyclohexane (●), 1,3-dimethylcyclohexane (■), and 1,3,5-trimethylcyclohexane (♦) reactants on 0.7 nm Ir clusters at 593 K. Dashed curves represent trends.

bonds) in CH, MCH, 1,3-DMCH, and 1,3,5-TMCH on 0.7 nm Ir clusters (20 kPa hydrocarbon, 593 K). These data are consistent with the rate equations derived for the case of hydrocarbon-saturated surfaces (eq 9) for H_2 pressures below 1 MPa and with those for H*-covered surfaces (eq 10) above 4 MPa H_2, which satisfies eq 11 for 20 kPa cycloalkane. The H_2 pressure required for H* to become MASI (eq 11) is higher for cyclohexanes with more methyl substituents. This trend reflects equilibrium constants for dehydrogenation and adsorption ($\Pi_{i=1}^{z} K_{CH,i} K_A$, eq 11) that also increase with increasing substitution because alkyl substituents introduce ^{3}C−H bonds that are weaker than ^{2}C−H bonds (by 8 kJ mol^{-1})[43] and therefore give rise to higher equilibrium coverages of dehydrogenated intermediates. A larger number of alkyl substituents also lead to lower total C−C cleavage (Figure 3) and ring-opening (Figure 4) rates for all H_2 pressures and a given temperature. C−C bond cleavage rates at endocyclic positions are 10−100 times larger, depending on H_2 pressure (0.2−5.5 MPa), for ^{2}C−^{2}C bonds in CH than for ^{3}C−^{2}C bonds in MCH, 1,3-DMCH, and 1,3,5-TMCH. These trends resemble the lower C−C rupture rates for ^{3}C−^{x}C bonds than for ^{2}C−^{2}C bonds as also found for the hydrogenolysis of acyclic isoalkanes.[18] These effects of methyl substituents (Figure 4) are also consistent with the reported preference for ring opening at C−C bonds containing less highly substituted C atoms in five-membered[1,5,6] and six-membered[1,3,4,8,28] alkyl-substituted cycloalkanes. These differences in rates reflect, in part, the larger λ values (by 0.5−1) for ^{3}C−^{x}C bond cleavage than for ^{2}C−^{2}C or ^{2}C−^{1}C bond cleavage within a given cycloalkane reactant. In the next section, we show that these larger λ values also lead to higher activation enthalpies ($\Delta H^{\ddagger}$) and entropies ($\Delta S^{\ddagger}$) for C−C bond cleavage and that such effects account for ring-opening rate constants that decrease monotonically with increasing substitution at endocyclic C atoms (Figure 4).

DOI: 10.1021/jp511688x
J. Phys. Chem. C 2015, 119, 2597−2613

3.3. C−C Bond Cleavage Transition States and Activation Enthalpies ($\Delta H^{\ddagger}$) and Entropies ($\Delta S^{\ddagger}$).

Equilibrated H* desorption and cycloalkane adsorption and dehydrogenation (steps 1.1−1.5, Scheme 1) form C−C cleavage transition states on H*-saturated surfaces and λ gaseous H_2 molecules. These transition states exist in equilibrium with their immediate precursors, in this case, $C_nH_{2n-y}(\gamma^*)$ species that are also in equilibrium with gaseous cyclohexanes and H_2 ($\eta_H \approx 1$, Figure 1). The combination of these equilibria leads to the stoichiometric equilibrated reaction

$$C_nH_{2n} + \gamma\, H(*) \overset{K'^{\ddagger}}{\rightleftharpoons} C_nH_{2n-y}(\gamma^*)^{\ddagger} + \lambda\, H_2 \qquad (12)$$

on H*-saturated surfaces. Here, $K'^{\ddagger}$ is the equilibrium constant for the formation of the transition state ($C_nH_{2n-y}(\gamma^*)^{\ddagger}$) and the evolution of λ H_2 molecules (where $\lambda = (\gamma + y)/2$).

The state function properties of free energies provide a rigorous strategy for expressing activation free energies ($\Delta G^{\ddagger}$) in terms of the properties of the catalysts and the molecules involved using Born−Haber thermochemical constructs (Scheme 2, depicting $^3C-^2C$ bond cleavage in MCH where y = 5 and γ = 3). These represent a sequence of hypothetical steps chosen for convenience because their thermodynamic properties are known[47] or can be determined from theory or experiment.[17] For the stoichiometric reaction represented by eq 12, these steps include the (i) dehydrogenation of a gaseous cycloalkane to form a gaseous form of the C_nH_{2n-y} intermediate (ΔG_D); (ii) desorption of γH* atoms to form the unoccupied sites required to bind C_nH_{2n-y} (ΔG_H); (iii) adsorption of the gaseous C_nH_{2n-y} species onto these sites (ΔG_A); and (iv) formation of the C−C cleavage transition state from the $C_nH_{2n-y}(\gamma^*)$ species (ΔG_R). The resulting $\Delta G^{\ddagger}$ values on H*-covered surfaces become

$$\Delta G^{\ddagger} = G^{\ddagger} + \lambda G_{H_2} - \gamma G_{H^*} - G_{C_nH_{2n}} \qquad (13)$$

Here, $G^{\ddagger}$ is the transition-state free energy, G_{H_2} and $G_{C_nH_{2n}}$ are the free energies of gaseous H_2(g) and C_nH_{2n}(g), respectively, and G_{H^*} is the free energy of chemisorbed H* at saturation coverages. Equation 13 shows that the $\Delta G^{\ddagger}$ values for cleaving a given C−C bond reflect the stability of the reactants (C_nH_{2n}(g); H*) and the products ($C_nH_{2n-y}(\gamma^*)^{\ddagger}$, H_2(g)) in eq 12 and the values of λ and γ for the required transition state.

The hydrogenolysis rate equation on H*-saturated surfaces (eq 10) can be restated through the formalism of transition-state theory by exploiting the equilibrated nature of eq 12 and expressing $\Delta G^{\ddagger}$ (Scheme 2) in terms of $\Delta H^{\ddagger}$ and $\Delta S^{\ddagger}$

$$\frac{r}{[L]} = \frac{k_B T}{h} K^{\ddagger} \frac{(C_nH_{2n})}{(H_2)^{\lambda}} = \frac{k_B T}{h} e^{\Delta S^{\ddagger}/R} e^{-\Delta H^{\ddagger}/RT} \frac{(C_nH_{2n})}{(H_2)^{\lambda}} \qquad (14)$$

where k_B and h are the Boltzmann and Planck constants, respectively. $K^{\ddagger}$ is the transition-state equilibrium constant determined from molecular partition functions (excluding the C−C bond vibration along the reaction coordinate that forms the transition state[16]). Thus, temperature effects on measured $K^{\ddagger}$ values (turnover rates for each distinct C−C cleavage divided by the number of such C−C bonds) give the $\Delta H^{\ddagger}$ and $\Delta S^{\ddagger}$ values for each distinct C−C bond in each cycloalkane reactant. Figure 5 shows $K^{\ddagger}$ values for the combined rate of C−C bond cleavage at all positions in MCH and *n*-PCH reactants and also in ethane and *n*-octane as a function of reciprocal temperature (0.7 nm Ir clusters saturated with H*). The $K^{\ddagger}$ values for each distinct C−C bond in these molecules (not shown) are used to estimate their respective $\Delta H^{\ddagger}$ and $\Delta S^{\ddagger}$

Scheme 2. Thermochemical Cycle Representing Free-Energy Changes for the Reaction Sequence (Scheme 1) that Forms C−C Bond Cleavage Transition States on H*-Covered Surfaces, Depicted Here for a Plausible Structure That Cleaves the $^3C-^2C$ Bond in Methylcyclohexane[a]

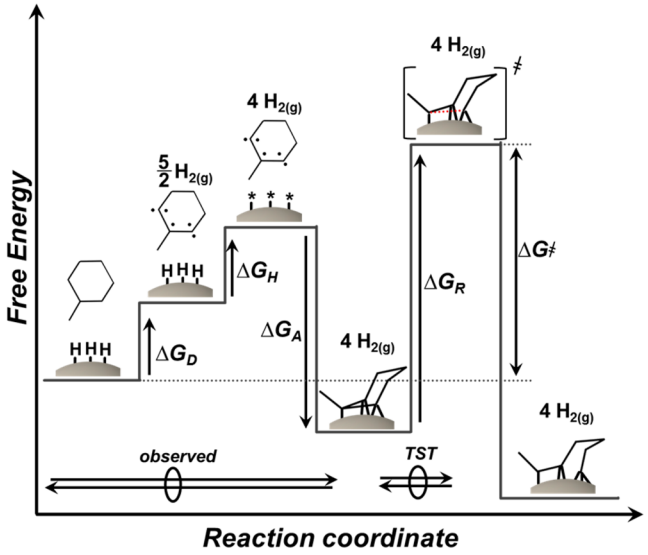

[a]Free-energy changes are shown for sets of steps that dehydrogenate the cycloalkane (ΔG_D), desorb γH* atoms (ΔG_H), adsorb the dehydrogenated cyclic hydrocarbon (ΔG_A), and rupture the C−C bond (ΔG_R). ⇄ plus ○ denotes quasi-equilibrated steps inferred from η_H values of unity or from transition-state theory (TST); the number of gas-phase H_2's indicated at each step is the total number formed during the sequence. Measured activation free energies ($\Delta G^{\ddagger}$) reflect the sum of the free-energy changes associated with all preceding steps and depend on the free energy of the transition state ($G^{\ddagger}$) and of gaseous H_2 (G_{H_2}) formed in the quasi-equilibrated reaction that forms the transition state (eq 12).

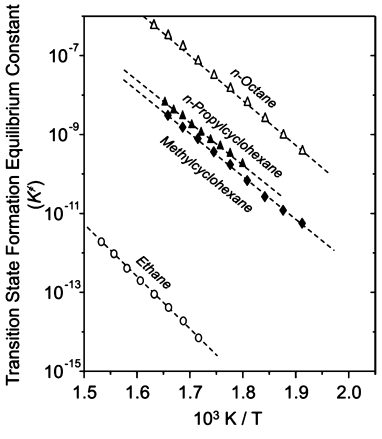

Figure 5. Eyring−Polanyi plot of $K^{\ddagger}$, the equilibrium constant for the formation of transition states and H_2 from the gas-phase cycloalkane reactant and the H*-covered metal surfaces (eq 12), as a function of inverse temperature for the conversion of alkyl cycloalkanes [methylcyclohexane (♦), *n*-propylcyclohexane (▲)] and acyclic *n*-alkanes [ethane (○) and *n*-octane (△)] on hydrogen-covered surfaces of 0.7 nm Ir clusters supported on silica. $K^{\ddagger}$ values for ethane and *n*-octane (ref 16) are shown for comparison to cycloalkanes, and dashed lines represent the regressed fits to the functional form of eq 14.

DOI: 10.1021/jp511688x
J. Phys. Chem. C 2015, 119, 2597−2613

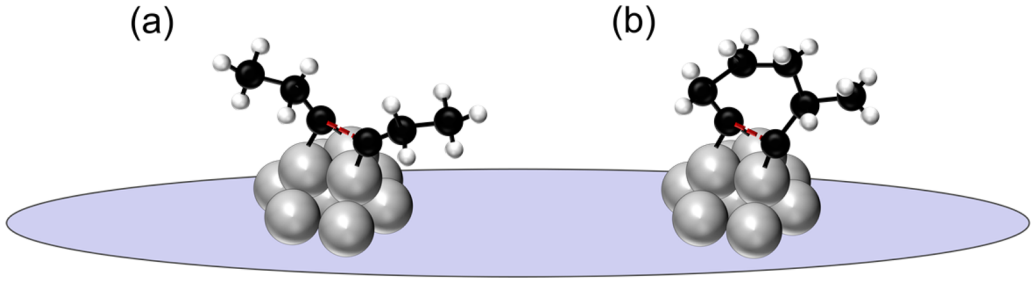

Figure 6. Schematic depiction of transition-state structures proposed for the cleavage of (a) central C−C bonds in *n*-hexane and (b) endocyclic ^{2}C−^{2}C bonds in methylcyclohexane on 0.7 nm Ir clusters. The transition states are depicted as tetra-σ bound species with α,β-coordination at the C atoms in the cleaved bond. The pendant alkyl chains in *n*-hexane are free to rotate, and each C−C bond can assume trans, gauche-, or gauche+ conformations, whereas the unbound C atoms in methylcyclohexane cannot rotate and different conformations of the C_6 ring are separated by energy differences much larger than k_BT.

values shown in Table 3. As shown below, these $\Delta H^{\ddagger}$ and $\Delta S^{\ddagger}$ values reflect the combined enthalpies and entropies of the steps in the hypothetical Born−Haber cycle depicted in Scheme 2.

The $\Delta H^{\ddagger}$ values for each C−C bond (Table 3) are given by the difference in enthalpy between the reactants and products involved in eq 12:

$$\Delta H^{\ddagger} = H^{\ddagger} + \lambda H_{H_2} - \gamma H_{H^*} - H_{C_nH_{2n}} \quad (15)$$

Differences in $\Delta H^{\ddagger}$ values among distinct C−C bonds on a specific surface are given solely by the term $(H^{\ddagger} - H_{C_nH_{2n}})$ because the other terms (H_{H^*} and H_{H_2}) do not depend on the identities of the cycloalkane reactants. These $(H^{\ddagger} - H_{C_nH_{2n}})$ terms depend, in turn, on BDE(C−C) values, on the number of H_2(g) molecules formed (λ, from alkylated cyclohexane dehydrogenation and H* desorption), and on the number of H*, each with enthalpy H_{H^*}, that desorb in order to bind the transition state (γ) on a given surface. The $\Delta H^{\ddagger}$ values (Table 3) range from 180 kJ mol^{-1} for ^{2}C−^{2}C bonds in *n*-PCH to 273 kJ mol^{-1} for ^{3}C−^{2}C bonds in MCH. The degree of unsaturation and the number of C−M bonds in the transition state are similar for cleaving ^{2}C−^{2}C, ^{2}C−^{1}C, and ^{1}C−^{1}C bonds, as evident from their similar λ values.[16−18] $\Delta H^{\ddagger}$ values and the binding modes of the transition states for ^{2}C−^{2}C and ^{2}C−^{1}C bond rupture in acyclic alkanes and cyclohexanes are similar, and differences among their $\Delta H^{\ddagger}$ values predominantly reflect differences in their BDE(C−C) values. For example, $\Delta H^{\ddagger}$ values for endocyclic ^{2}C−^{2}C bonds in MCH (204−211 kJ mol^{-1}, Table 3) resemble those for ^{2}C−^{2}C bonds in *n*-hexane (217 kJ mol^{-1}[16]) because BDE(^{2}C−^{2}C) values for *n*-hexane and cyclohexanes[14] and the extent of dehydrogenation and number of sites required for these two reactants (γ = 4 and γ = 2, based on $\lambda \approx 3$ for ^{2}C−^{2}C bonds in *n*-hexane[16] and MCH, Table 3) are similar in these tetra-σ α,β-bound transition states.

In contrast, $\Delta H^{\ddagger}$ values for ^{3}C−^{1}C (240 kJ mol^{-1}, MCH) and ^{3}C−^{2}C (236 kJ mol^{-1}, *n*-PCH; 273 kJ mol^{-1}, MCH) bonds are larger (by 30−55 kJ mol^{-1}) than for endocyclic ^{2}C−^{2}C bonds within the same molecule (Table 3), even though BDE(^{3}C−^{x}C) values are smaller than BDE(^{2}C−^{2}C) values. Alkyl substituents at C−C bonds in cyclic and acyclic alkanes lead to higher $\Delta H^{\ddagger}$ values because ^{3}C atoms cannot bind to surfaces via di-σ bonds, which facilitate electron transfer to antibonding C−C orbitals,[18,26,27,32] whereas ^{2}C atoms can bind in such configurations by forming multiple bonds to exposed metal atoms at catalytic surfaces.[17,22,35,44,48] These differences in binding modes between ^{3}C−^{x}C and ^{2}C−^{2}C rupture transition states lead to their significantly different $\Delta H^{\ddagger}$ values, which reflect the additional endothermic H* desorption and C−H rupture events needed for ^{3}C−^{x}C cleavage transition states ($\gamma \geq 3, y \geq 4$) in comparison to ^{2}C−^{2}C rupture transition states ($\gamma = 2, y = 4$). These larger $\Delta H^{\ddagger}$ values for ^{3}C−^{x}C bonds show that the enthalpy of the additional H-removal steps is not fully compensated for by the exothermic formation of the new C−M bonds.[18] These mechanistic interpretations account for λ and $\Delta H^{\ddagger}$ values that are larger for the hydrogenolysis of C−C bonds at the most substituted positions in both alkyl cyclohexanes (Table 3) and acyclic isoalkanes,[18] and such seemingly general trends indicate that these concepts also account for different values for $\Delta H^{\ddagger}$ and rate constants for C−C cleavage at substituted and unsubstituted positions in other cycloalkane reactants (e.g., cyclopentanes and polycyclic species) and on other catalytic surfaces (e.g., Ru,[1,18] Rh,[18,27,49] Ni,[1] and Pt[1,6,18,27]).

C−C bond cleavage events involve large and positive activation entropies for cyclic and acyclic alkanes ($\Delta S^{\ddagger}$ = 143−302 J mol^{-1} K^{-1} in cyclohexanes, Table 3, and 164−268 J mol^{-1} K in acyclic alkanes[16,18]); these entropy gains make it possible for these reactions to occur at detectable rates in spite of their very large $\Delta H^{\ddagger}$ values (Table 3). These entropy gains are made possible by the evolution of λ moles of H_2(g) upon formation of the hydrogenolysis transition state (eq 12) on H*-covered surfaces:

$$\Delta S^{\ddagger} = S^{\ddagger} + \lambda S_{H_2} - \gamma S_{H^*} - S_{C_nH_{2n}} \quad (16)$$

This equation parallels that for enthalpies (eq 15) and accounts for the entropy changes in each step of the Born−Haber cycle depicted in Scheme 2. The values of S_{H_2} (134−132 J mol^{-1} K^{-1}, 3−4 MPa H_2, respectively) and $S_{C_nH_{2n}}$ (500−620 J mol^{-1} K^{-1} for gaseous MCH and *n*-PCH, at 10 kPa cycloalkanes, 593 K) can be obtained from tabulated data at their standard state (1 bar, 298 K[47]). The S_{H^*} value for chemisorbed hydrogen atoms (35 J mol^{-1} K^{-1} at 593 K) was estimated from statistical mechanics treatments for 2D ideal gases at saturation coverages (i.e., H*/M$_s$ = 1).[50] These data and estimates, taken together with measured $\Delta S^{\ddagger}$ values for each C−C bond (Table 3), can then be used to calculate $S^{\ddagger}$ values using eq 16. Below, we compare these measured $S^{\ddagger}$ values to estimates from statistical mechanics descriptions of plausible transition-state structures to assess the reasonableness of the elementary steps (Scheme 1) and the relevant transition states and our mechanistic interpretation (Scheme 2) of hydrogenolysis rate data.

DOI: 10.1021/jp511688x
J. Phys. Chem. C 2015, 119, 2597−2613

The $S^{\ddagger}$ values for C−C cleavage in cyclic and acyclic alkanes can be estimated from molecular partition functions[51] that describe each degree of freedom in a postulated transition-state structure; these include 2D frustrated translations ($S^{\ddagger}_{2D,trans}$), intramolecular vibrations ($S^{\ddagger}_{vib}$), rigid rotations of any free alkyl chains ($S^{\ddagger}_{1D,rot}$), and conformational changes about each C−C bond ($S^{\ddagger}_{conf}$).[16−18] Transition states for cleaving ^{2}C−^{2}C and ^{2}C−^{1}C bonds consist of tetra-σ α,β-bound structures[16,17,22,48] because three H_2 molecules ($\lambda = 3$) are evolved upon formation of transition states that contain four fewer H atoms than alkane reactants ($y = 4$) and are bound to two vicinal sites ($\gamma = 2$), as shown for *n*-alkanes.[16,17] The $S^{\ddagger}$ values for ^{3}C−^{x}C bond cleavage transition states in alkyl cyclohexanes (and acyclic isoalkanes[18]) are smaller than for the cleavage of ^{2}C−^{2}C or ^{2}C−^{1}C bonds in the same molecule because the ^{3}C−^{x}C bond cleavage transition states contain three or more C atoms that must dehydrogenate and bind to the metal surface ($\gamma \geq 3$), thus decreasing $S^{\ddagger}_{1D,rot}$ (by decreasing the length of any free alkyl chains) and, to a lesser extent, $S^{\ddagger}_{2D,trans}$ (multiple attachments increase the frequency of frustrated translations) values.[18]

The cyclic structure of alkyl cyclohexanes leads to smaller $S^{\ddagger}$ values for cyclohexane-derived surface complexes than for acyclic alkanes with similar carbon numbers because the C_6-ring structures restrict rotations and provide fewer stable conformations at the transition state.[14] Pendant alkyl chains in adsorbed species formed from acyclic alkanes rotate freely in C−C bond cleavage transition states; these rotational modes account for 40−70 J mol^{-1} K^{-1} of the entropy in acyclic C_6−C_8 alkanes.[16,18] In contrast, such chains are connected via the ring structure in transition states for endocyclic C−C bond cleavage (Figure 6); as a result, rotational modes ($S^{\ddagger}_{1D,rot}$) do not contribute to the entropy of endocyclic cleavage transition states.

C_6-ring structures also exhibit fewer stable conformations than for acyclic alkanes with similar carbon numbers because their conformations differ in energy by much more than RT and such modes become inaccessible at hydrogenolysis temperatures (e.g., at 593 K, chair conformations in cyclohexanes are more stable than other conformations by $\Delta H/RT > 4.5$;[14] whereas trans and gauche conformations in *n*-alkanes differ by $\Delta H/RT = 0.5$[52]). As a result, $S^{\ddagger}_{conf}$ values are 15−25 J mol^{-1} K^{-1} smaller for C_6−C_9 cycloalkanes than for C_6−C_9 *n*-alkanes. Taken together with low values of $S^{\ddagger}_{1D,rot}$ for cyclohexanes, these lower $S^{\ddagger}_{conf}$ values lead to $S^{\ddagger}$ estimates that are 60−100 J mol^{-1} K^{-1} smaller for alkyl cyclohexanes than for acyclic alkanes with the same number of carbon atoms. These differences in $S^{\ddagger}$ values for cyclic and acyclic transition states (60−100 J mol^{-1} K^{-1}) resemble similar reported differences between entropies of gaseous cyclic and acyclic alkane molecules (e.g., $S_{n\text{-heptane,593 K}} - S_{MCH,593\ K} = 98$ J mol^{-1} K^{-1}, $S_{n\text{-nonane,593 K}} - S_{n\text{-PCH,593 K}} = 100$ J mol^{-1} K^{-1} [47]), whose entropies also differ because of the fewer rotational modes and configurations for cyclic species. As a result, the difference between the entropy of ^{3}C−^{x}C or ^{2}C−^{2}C rupture transition states and their respective gas-phase alkanes (i.e., $S^{\ddagger} - S_{C_nH_{2n}}$) are similar for cyclic and acyclic reactants.

Figure 7 compares measured $S^{\ddagger}$ values and those determined from statistical mechanics estimates for cyclohexanes (MCH, *n*-PCH), isoalkanes (isobutane, 2-methylpentane),[18] and *n*-alkanes (C_2−C_8).[16,17] The measured $S^{\ddagger}$ values are calculated from $\Delta S^{\ddagger}$ values (Table 3) using eq 16, with λ values from Table 3 and the restriction that $y \geq \gamma$, which ensures that

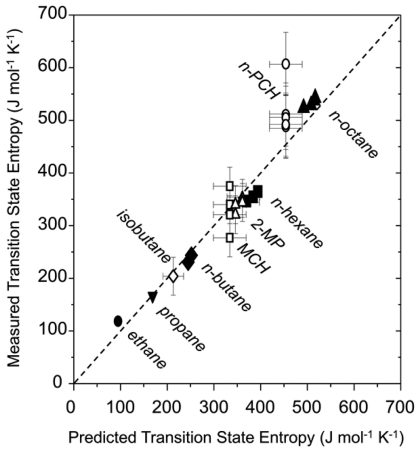

Figure 7. Measured and predicted transition-state entropies for cleaving C−C bonds in cycloalkanes, isoalkanes (adapted from ref 18), and *n*-alkanes (adapted from ref 16). Values from H*-covered surfaces of 0.7 nm Ir clusters, 593 K (ethane (●), propane (▼), isobutane (◊), *n*-butane (♦), methylcyclohexane (□), 2-methylpentane (△), *n*-hexane (■), *n*-propylcyclohexane (○), and *n*-octane (▲)). One point is shown for each distinguishable C−C bond in every alkane. Uncertainty bars for *n*-alkanes are ±5 J mol^{-1} K^{-1} and are not visible; uncertainties for isoalkane and cyclohexane transition-state entropies are larger (>±35 J mol^{-1} K^{-1}) because of the greater uncertainties in λ values used to calculate transition-state entropies (eq 16).

transition-state structures are consistent with measured rate data and the principles of bond order conservation. $S^{\ddagger}$ values for MCH and *n*-PCH are estimated from statistical mechanics with the assumptions that they possess no rotational entropy (i.e., $S^{\ddagger}_{1D,rot} = 0$) and that $S^{\ddagger}_{2D,trans}$, $S^{\ddagger}_{vib}$, and $S^{\ddagger}_{conf}$ are identical for all C−C rupture transition states for a given alkyl cyclohexane reactant. The uncertainties in the $S^{\ddagger}$ values of the ordinate, determined using measured $\Delta S^{\ddagger}$ values, reflect the combined uncertainties in $\Delta S^{\ddagger}$ and λ values; the abscissa uncertainties, determined using statistical mechanics reflect only those in λ estimates (Table 2). For both axes, the uncertainties are greater for cyclohexanes than for *n*-alkanes or isoalkanes because the hydrogenolysis of cyclic reactants gave higher selectivities to multiple hydrogenolysis products, which may form via an initial C−C bond rupture at several different locations in the cycloalkane reactants. Nevertheless, calculated and measured $S^{\ddagger}$ values are in excellent agreement for both acyclic and cyclic alkanes (Figure 7, correlation has a slope of 1.03 ± 0.10), suggesting that the proposed pathways (Schemes 1 and 2) and the corresponding postulated transition-state structures seem to accurately reflect those actually involved in the hydrogenolysis of cyclic and acyclic alkanes.

The $S^{\ddagger}$ values for alkanes (Figure 7, cyclic and acyclic) reflect their respective transition-state structures, which depend on the number and the location of surface attachments in the transition state. Increase in the number of H_2 molecules formed (λ) increases $\Delta S^{\ddagger}$ directly (eq 16) but influences $S^{\ddagger}$ only indirectly by forming more surface attachments, which lead to less translational freedom in the transition state. These $S^{\ddagger}$ values increase monotonically with increasing chain length for *n*-alkanes because the mass and the number of degrees of freedom of the transition state concomitantly increase.[16] Figure 7 shows that among alkanes with identical numbers of C atoms, $S^{\ddagger}$ values for ^{3}C−^{x}C cleavage transition states are smaller than for ^{2}C−^{2}C or ^{2}C−^{1}C rupture (e.g., $S^{\ddagger}_{n\text{-butane}} > S^{\ddagger}_{isobutane}$) in acyclic alkanes, and more substituted C−C bonds involve

DOI: 10.1021/jp511688x
J. Phys. Chem. C 2015, 119, 2597−2613

transition states with more C−M bonds, which restricts their rotation and translation and lead to smaller $S^{\ddagger}$ values. The $S^{\ddagger}$ values for C−C cleavage at all positions in cycloalkanes are even lower than for both acyclic *n*-alkanes and isoalkanes of the same carbon number (Figure 7) because the C_6 ring restricts both rotational motion and conformational modes. For example, although MCH contains more C atoms and exhibits more degrees of freedom than *n*-hexane or 2-methylpentane, its $S^{\ddagger}$ value is smaller (Figure 7). Similarly, transition states that mediate C−C bond cleavage in *n*-PCH exhibit $S^{\ddagger}$ values smaller than those for *n*-octane (Figure 7). Measured $S^{\ddagger}$ values for most C−C bonds in a given cycloalkane are similar (within the uncertainties for MCH and *n*-PCH shown in Figure 7). Exocyclic $^{2}C-^{2}C$ bond rupture in *n*-PCH (i.e., deethylation), however, gives measured $S^{\ddagger}$ values of 607 ± 60 J mol^{-1} K^{-1}; these are ∼100 J mol^{-1} K^{-1} larger than for all other C−C bonds in *n*-PCH. This large $S^{\ddagger}$ value for deethylation reflects the uncertainties brought forth by the prevalence of multiple hydrogenolysis products with such reactants, which reflect initial C−C bond ruptures at uncertain locations.

3.4. C−C Bond Cleavage Locations in Cyclohexanes and the Influence of Ir Cluster Size. Differences in the number of surface attachments (γ) and of H atoms removed (y) among transition states for C−C cleavage at different locations in cyclic alkanes (e.g., endocyclic $^{3}C-^{2}C$ or $^{2}C-^{2}C$ bonds) account for previously observed effects of temperature and H_2 pressure on ring-opening products.[1,4,6,8,11,53] The ratios of rates for C−C bond cleavage at unsubstituted ($^{2}C-^{2}C$, $^{2}C-^{1}C$) and substituted ($^{3}C-^{x}C$) positions in cyclohexanes are given by

$$\chi = \frac{r_{^{2}C-^{2}C} + r_{^{2}C-^{1}C}}{r_{^{3}C-^{x}C}} \quad (17)$$

Here, each r_{xC-yC} represents the rate of $^{x}C-^{y}C$ bond cleavage normalized by the number of distinct $^{x}C-^{y}C$ bonds in each reactant. Figure 8a shows that χ values, and thus the selectivities to branched alkane products, increase with increasing H_2 pressure (0.15−5.5 MPa) for MCH, 1,3-DMCH, and *n*-PCH because $^{3}C-^{x}C$ rupture transition states are more dehydrogenated and also require more binding sites (λ = 2.4−4.1, eq 14, Table 3) than those for $^{2}C-^{2}C$ and $^{2}C-^{1}C$ cleavage (λ = 1.5−3.0, eq 14, Table 3). As a result, the number of $^{3}C-^{x}C$ cleavage transition states decreases more strongly with increasing H_2 pressure than for those mediating C−C cleavage at less substituted positions (i.e., $^{2}C-^{2}C$ and $^{2}C-^{1}C$); these results and arguments are consistent also with the reported effects of H_2 pressure on χ values for acyclic alkanes.[18]

The loss of carbon atoms in the ring opening of alkyl cyclohexanes becomes smaller with the increasing ratio of rates for endocyclic and exocyclic C−C cleavage

$$\beta = \frac{r_{endo,C-C}}{r_{exo,C-C}} \quad (18)$$

where $r_{endo,C-C}$ and $r_{exo,C-C}$ are the C−C rupture rates at endocyclic and exocyclic positions, respectively, and where each rate is normalized by the number of such C−C bonds in the reactant. Figure 8b shows that increasing H_2 pressures lead to larger β values for all alkyl cyclohexanes containing endocyclic $^{2}C-^{2}C$ bonds (MCH, 1,3-DMCH, *n*-PCH). The β values at each H_2 pressure are similar for methyl-substituted cyclohexanes (MCH, 1,3-DMCH, Figure 8b), but β is smaller for the cyclohexanes with longer substituents (e.g., *n*-PCH) than for those with shorter ones (e.g., MCH, Figure 8b). These trends in β values among cyclohexanes show that ring-opening selectivities (defined as the fraction of converted reactant that forms acyclic products with the same number of C atoms as the cyclic reactant) decrease with increasing numbers of alkyl substituents on the ring. Ring-opening selectivities decrease as the length of *n*-alkyl groups increases because of a concomitant increase in the number of exocyclic $^{2}C-^{2}C$ and $^{2}C-^{1}C$ bonds (e.g., 0 for MCH, 2 for *n*-PCH). These less-substituted C−C bonds cleave more readily because they require fewer binding sites to stabilize dealkylation transition states than do those that cleave $^{3}C-^{x}C$ bonds. The ratios of rates for endocyclic and exocyclic $^{3}C-^{x}C$ bond cleavage in substituted cycloalkanes, however, do not change with H_2 pressure because λ values are similar (within ±0.3, Table 3) for a given alkyl cyclohexane. The data in Figure 8 shows that ring-opening selectivities and the extent of branching in the acyclic alkanes formed both depend sensitively on H_2 pressure because the extent of dehydrogenation (y) and the number of surface attachments (γ) differ among the transition states that form the branched and linear alkane products.

The differences in y and γ values among these transition states cause the relative rates of C−C cleavage at substituted and unsubstituted positions to also depend on reaction temperature. Figure 9a shows χ values that increase with

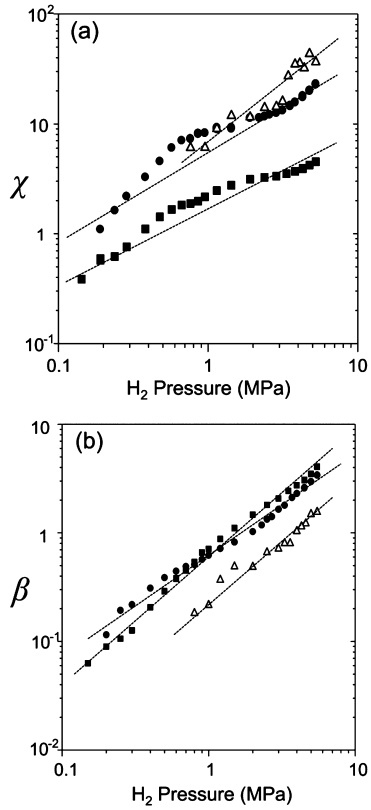

Figure 8. Effects of H_2 pressure on (a) the ratio of the rate of C−C bond cleavage at unsubstituted ($^{2}C-^{2}C$, $^{2}C-^{1}C$) positions normalized by the number of these bonds in the reactant to that at substituted positions ($^{3}C-^{2}C$, $^{3}C-^{1}C$) (χ) and (b) the ratio of the rate of ring opening, normalized by the number of endocyclic C−C bonds, to the rate of dealkylation, normalized by the number of exocyclic C−C bonds (β). Data are shown for MCH (●), 1,3-DMCH (■), and *n*-PCH (△) as a function of H_2 pressure on 0.7 nm Ir clusters for 20 kPa cycloalkanes and 593 K. Lines are trends.

DOI: 10.1021/jp511688x
J. Phys. Chem. C 2015, 119, 2597−2613

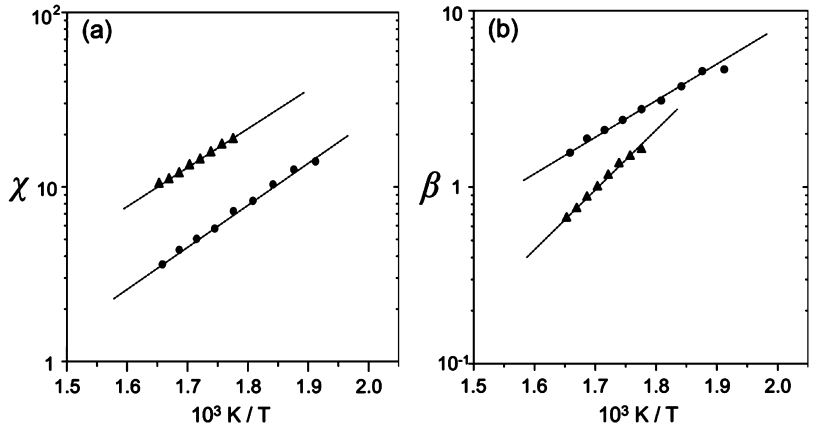

Figure 9. Temperature effects on (a) the ratio of the rate of C−C bond cleavage at unsubstituted (^{2}C−^{2}C, ^{2}C−^{1}C) positions normalized by the number of these bonds in the reactant to that at substituted positions (^{3}C−^{2}C, ^{3}C−^{1}C) (χ) and (b) the ratio of the rate of ring opening, normalized by the number of endocyclic C−C bonds, to the rate of dealkylation, normalized by the number of exocyclic C−C bonds (β), for methylcyclohexane (●, 10 kPa MCH, 3.5 MPa H_2) and *n*-propylcyclohexane (▲, 10 kPa *n*-PCH, 4.0 MPa H_2) on 0.7 nm Ir clusters. Dashed lines represent exponential fits to χ and β values as a function of inverse temperature.

decreasing temperature for MCH and *n*-PCH reactants on H*-covered Ir surfaces. These trends reflect the larger $\Delta H^{\ddagger}$ values for ^{3}C−*C than for ^{2}C−^{2}C or ^{2}C−^{1}C cleavage for a given cycloalkane (by 15−70 kJ mol^{-1}, Table 3). The larger $\Delta H^{\ddagger}$ values for ^{3}C−*C bonds (vs ^{2}C−^{2}C or ^{2}C−^{1}C bonds) reflect ^{3}C−*C cleavage transition states that require the removal of more H atoms from the cycloalkane and the H*-covered surface than for ^{2}C−^{2}C or ^{2}C−^{1}C cleavage transition states.[17,22] These additional H-removal steps are endothermic and reflect the relative energies of the C−H and M−H bonds broken and of the C−M bonds formed, as discussed in section 3.3.

The β values (Figure 9b) increase with decreasing temperature because endocyclic C−C bond cleavage in singly substituted cyclohexanes (e.g., MCH and *n*-PCH) has smaller $\Delta H^{\ddagger}$ values (because of their lesser C atom substitution) than the exocyclic C−C bonds. These different $\Delta H^{\ddagger}$ values for cleaving substituted and unsubstituted C−C bonds lead to hydrogenolysis selectivities that depend sensitively on temperature for alkyl cyclohexanes.

$\Delta H^{\ddagger}$ values for C−C rupture depend on the enthalpy of hydrogen adsorption (H_{H^*}, where $H_{H^*} < 0$, eq 15) because it determines the enthalpy change of forming vacancies required to bind the transition states ($^1/_2H_{H_2} - H_{H^*}$). Figure 10 shows that $\Delta H^{\ddagger}$ values for MCH hydrogenolysis are smaller (and turnover rates are larger) on H*-saturated surfaces of large Ir clusters (7 nm) than of smaller Ir clusters (2.7 and 0.7 nm). Measured $\Delta H^{\ddagger}$ values for the total rate of MCH hydrogenolysis (the combined C−C rupture rates at all positions, eq 15) are smaller on larger clusters (212 kJ mol^{-1} on 0.7 nm Ir; 174 kJ mol^{-1} on 2.7 nm Ir; and 132 kJ mol^{-1} on 7 nm Ir). Table 4 shows that $\Delta H^{\ddagger}$ values for C−C bond cleavage at each distinct position in MCH also decreases systematically with increasing Ir cluster size. These Ir cluster size differences (0.7−7 nm) can influence $\Delta H^{\ddagger}$ (eq 15) only through changes in the properties of the adsorbed species (i.e., $H^{\ddagger}$ and H_{H^*}) because those for gaseous reactants ($H_{C_nH_{2n}(g)}$) and products ($H_{H_2(g)}$) are unaffected by the nature and binding properties of catalyst surfaces. Microcalorimetry has shown that the heat of dissociative H_2 adsorption decreases with increasing Ir cluster size (1−10 nm)[54,55] and that H* binds 15−25 kJ mol^{-1} more strongly on edge and corner atoms prevalent on smaller clusters

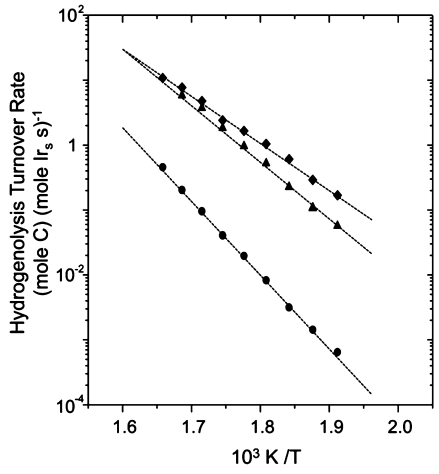

Figure 10. Methylcyclohexane (MCH) hydrogenolysis turnover rates as a function of reciprocal temperature on H*-saturated surfaces of Ir clusters with mean cluster sizes (from H_2 uptakes) of 0.7 nm (●), 3 nm (▲), and 7 nm (♦) for 10 kPa MCH and 3.5 MPa H_2. Dashed lines represent exponential fits to turnover rates as a function of reciprocal temperature.

(~1 nm) than on terrace sites (>10 nm) at near-saturation surface coverages (e.g., $1 \leq H^*/Ir_s \leq 1.5$).[54,55] Consequently, the process of generating vacancies, required to bind a transition state, is more endothermic on the surfaces of small clusters than it is for large clusters. Prevalent descriptions for the binding of adsorbed species on metal surfaces suggest that as the size of Ir clusters decreases, the stability of H* will increase, as will the stability of hydrogenolysis transition states that bind via C−M bonds.[56] The differences between $\Delta H^{\ddagger}$ values on small (0.7 nm) and large (7 nm) Ir clusters reflect changes in the quantity $H^{\ddagger} - \gamma H_{H^*}$ (eq 16), which reflect the strengths of C−M and H−M bonds, respectively. $\Delta H^{\ddagger}$ values on large Ir clusters (7 nm) are smaller for all C−C bonds in MCH (by 70−90 kJ mol^{-1}) than those on the smaller Ir clusters (0.7 and 2.7 nm). These trends in $\Delta H^{\ddagger}$ values with cluster size (Table 4) show that the enthalpic stability of the 2−3 H*'s that must be desorbed decreases more than that of the transition state itself (Scheme 2) as a result of the greater coordinative saturation of exposed atoms on larger clusters.[57]

DOI: 10.1021/jp511688x
J. Phys. Chem. C 2015, 119, 2597−2613

Table 4. $\Delta H^{\ddagger}$ Values for the Cleavage of the Indicated C−C Bonds in Methylcyclohexane on Hydrogen-Covered Surfaces of 0.7, 3, and 7 nm Ir Clusters

C-C Bond	$\Delta H^{\ddagger}$ (kJ mol^{-1})		
	0.7 nm Ir	3 nm Ir	7 nm Ir
	204	165	117
	211	184	139
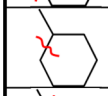	273	250	193
	240	187	150

These unequal effects of cluster size on the stability of the γH* desorbed and the transition state formed also cause the size of Ir clusters to affect the position of C−C rupture in alkyl cyclohexanes. The selectivity toward ^{2}C−^{2}C (χ, Figure 11a) and ring opening (β, Figure 11b) in MCH are highest on small Ir clusters (0.7 nm). The values of χ and β are also most sensitive to temperature on small clusters (Figure 11) because these small clusters give the greatest differences between the enthalpies of H* atoms and C−C rupture transition states. The effect of temperature on χ (Figure 11a) show that the enthalpic preferences for ^{2}C−^{2}C over ^{3}C−^{x}C bond cleavage are larger for smaller clusters (43 kJ mol^{-1} for 0.7 nm Ir; 25 kJ mol^{-1} for 7 nm Ir) because the additional H* atom desorption and surface attachment formation steps required for ^{3}C−^{x}C rupture, compared to those for ^{2}C−^{2}C cleavage (eq 15), are more endothermic on small (0.7 nm) Ir clusters than they are on large (7 nm) clusters. Both the differences between $\Delta H^{\ddagger}$ values for ^{3}C−^{x}C and ^{2}C−^{2}C bond cleavage and differences in the sensitivity of their $\Delta H^{\ddagger}$ values to cluster size result from the dissimilar binding configurations and site requirements associated with their respective transition-state structures.

These data show the effects of H_2 pressure, temperature, and Ir cluster size on C−C rupture rates and selectivities during ring-opening hydrogenolysis. The conclusions drawn from their mechanistic interpretation provide useful guidance for how reaction conditions and catalyst cluster diameters can be modified to control carbon losses and product quality. The preferred location of C−C cleavage reflects intrinsic differences between how ^{3}C atoms and ^{2}C atoms (or ^{1}C atoms) bind to catalytic surfaces; ^{3}C atoms of alkanes have a single C−H bond and can form a single attachment to catalytic surfaces whereas ^{2}C atoms can lose two H atoms and form two C−M bonds. This difference requires that ^{3}C−^{x}C rupture transition states for alkyl cyclohexanes form by desorbing more H* atoms, cleaving more C−H bonds, and binding more C atoms than those for ^{2}C−^{2}C and ^{2}C−^{1}C bonds. Differences among the rates and λ, $\Delta H^{\ddagger}$, and $\Delta S^{\ddagger}$ values for ^{3}C−^{x}C rupture and those for ^{2}C−^{2}C and ^{2}C−^{1}C rupture in alkyl cycloalkanes are similar to the differences seen for acyclic isoalkanes,[18] which shows that the effects of C-atom substitution on transition-state structures and

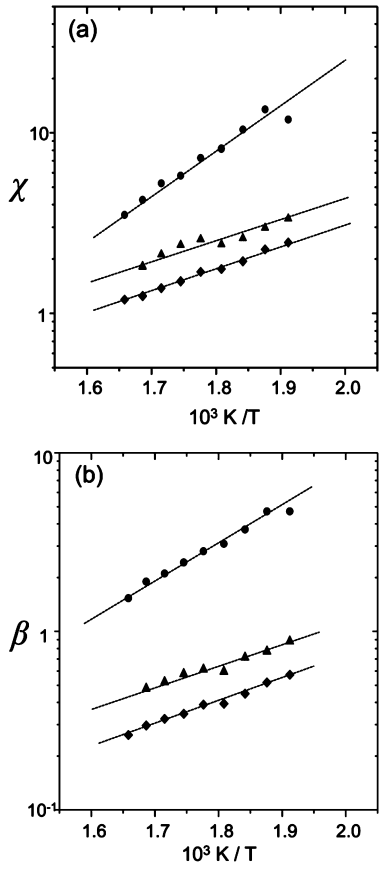

Figure 11. Temperature effects on (a) the ratio of the rate of C−C bond cleavage at unsubstituted (^{2}C−^{2}C, ^{2}C−^{1}C) positions normalized by the number of these bonds in the reactant to that at substituted positions (^{3}C−^{2}C, ^{3}C−^{1}C) (χ) and (b) the ratio of the rate of ring opening, normalized by the number of endocyclic C−C bonds, to the rate of dealkylation, normalized by the number of exocyclic C−C bonds (β), for methylcyclohexane (MCH) on H*-saturated surfaces of 0.7 nm (●), 3 nm (▲), and 7 nm (♦) Ir clusters for 10 kPa MCH and 3.5 MPa H_2. Dashed lines represent exponential fits to χ and β values as a function of inverse temperature.

stabilities are general for hydrogenolysis reactions of alkanes. Moreover, the hydrogenolysis of acyclic isoalkanes shows identical trends in these parameters among metal clusters with different elemental identities (Ir, Ru, Rh, and Pt) and size (0.7−7 nm),[18] indicating that the mechanistic details we have described are largely independent of the composition and diameter of catalytic clusters. Rates and selectivities for the hydrogenolysis of branched,[18] unbranched,[16,17] and cyclic and acyclic alkanes are accurately described using an identical set of elementary steps (Scheme 1) with only minor changes to account for differences in the extent of dehydrogenation and the number of surface attachments of the transition state for distinct C−C bonds. Thus, it seems likely that the principles developed in this study and the preceding publications[16−18] are broadly applicable to metal-catalyzed alkane hydrogenolysis reactions. We expect that these concepts also extend to the cleavage of C−X bonds (where X = S, N, or O atoms) within cyclic and acyclic organic molecules because differences between the number of easily removed H atoms that each C, S, N, or O atom possesses in the cleaved bond will determine the number of surface attachments needed to bind these transition states during hydrodesulfurization, hydrodenitrogenation, and hydrodeoxygenation reactions on metal clusters.

DOI: 10.1021/jp511688x
J. Phys. Chem. C 2015, 119, 2597−2613

For example, the explanations presented here are consistent with C−S bond rupture rates that are lower for dibenzothiophenes than for thiophene[58] because ^{3}C−S bond rupture in the former is likely to require binding the transition state to the surface through more attachments than ^{2}C−S cleavage in thiophene and consequently give greater activation enthalpies on H*-covered surfaces. Thus, these concepts illustrated here may also help to guide the design of catalytic conditions and materials for selective hydrotreating reactions.

4. CONCLUSIONS

Rates of C−C bond cleavage in differently alkylated cyclohexanes (C_7−C_9) measured as functions of reactant pressures and temperature are used to show how the stability of C−C rupture transition states depends on the structure of the reactants and the size of the Ir clusters. The transition states for C−C rupture in cyclohexanes form via equilibrated dehydrogenation reactions that break C−H bonds, form C−metal bonds, and desorb H* from the H*-saturated surfaces of Ir clusters. These steps form λH_2(g) molecules that are equilibrated with the transition state for C−C rupture, the gas-phase reactant, and the H*-covered Ir surface. In nearly all cases (except the deethylation of *n*-PCH) ^{3}C−^{x}C bond rupture involves larger $\Delta H^{\ddagger}$, $\Delta S^{\ddagger}$, and λ values than ^{2}C−^{2}C and ^{2}C−^{1}C cleavage. These differences show that dealkylation or ring opening via ^{3}C−^{x}C bond cleavage requires deeper dehydrogenation of the substituted cyclohexane and more surface attachments than needed for ^{2}C−^{2}C rupture. Consequently, an endothermic sequence of steps (C−H bond rupture, H* desorption, and C−M bond formation) must occur several more times to bind ^{3}C−^{x}C rupture transition states, and these additional steps increase $\Delta H^{\ddagger}$ values. These same steps, however, also produce additional H_2(g), giving larger λ values (by 0.5−1) as well as larger $\Delta S^{\ddagger}$ values (by 80−110 J mol^{-1} K^{-1}) for ^{3}C−^{x}C bond cleavage compared to values for ^{2}C−^{2}C and ^{2}C−^{1}C rupture. Comparisons between measured $S^{\ddagger}$ values and $S^{\ddagger}$ values predicted from statistical mechanics descriptions of cycloalkane-derived transition states show that these complexes possess less entropy than transition states for acyclic alkanes because the cyclic nature of these structures significantly reduces rotational and conformational entropy as also seen in comparisons between the entropies of gaseous cyclic and acyclic alkanes. $\Delta H^{\ddagger}$ for C−C cleavage in all reactants reflects, in part, the enthalpy of the H* atoms that are desorbed to bind the transition state and the strength of C−M bonds that bind transition states to the surface. Thus, differences between C−C cleavage rates and $\Delta H^{\ddagger}$ values on Ir clusters of different average sizes show that γH_{H^*} and $H^{\ddagger}$ differ in their sensitivity to changes in the average undercoordination of the Ir cluster surfaces. The largest Ir clusters (7 nm) give higher rates and lower $\Delta H^{\ddagger}$ values because high coordination terraces of large Ir clusters bind the γH* atoms more weakly than the undercoordinated surfaces of small clusters (<1 nm), and these differences are not fully compensated by commensurate changes in the strength of C−M bonds. The ratio of the rates of ^{2}C−^{2}C rupture to ^{3}C−^{x}C rupture and ring opening selectivities also depend on the size of Ir clusters because of these disproportionate changes in γH_{H^*} and $H^{\ddagger}$ with the size of Ir clusters. $\Delta H^{\ddagger}$ for transition states that bind the greatest number of C atoms to the surface (e.g., those for ^{3}C−^{x}C rupture) have the greatest absolute value for the term γH_{H^*} and are therefore most sensitive to the stability of H* atoms and the size of catalytic metal clusters. These data and their interpretation provide insight for the development of catalysts and processes that seek to hydrogenate polyaromatic hydrocarbons and subsequently cleave specific C−C bonds to form linear or branched alkane fuels; these results also seem to be relevant for understanding the processes that rupture C−O, C−S, and C−N bonds to remove heteroatoms via hydrotreating reactions.

■ ASSOCIATED CONTENT

Supporting Information

Representative transmission electron micrographs and cluster diameter distributions of the Ir−SiO_2 catalysts. This material is available free of charge via the Internet at http://pubs.acs.org

■ AUTHOR INFORMATION

Corresponding Author

*Fax: + 1 510 642 4778. E-mail: iglesia@berkeley.edu.

Present Address

(A.U.) Department of Chemical and Biological Engineering, Koç University, Istanbul, Turkey.

Notes

The authors declare no competing financial interest.

■ ACKNOWLEDGMENTS

We acknowledge Dr. Elif Gürbüz for assistance in taking the data and helpful discussions, Dr. Chris Kliewer (ExxonMobil) for obtaining the TEM images and particle size statistics, and Dr. Stuart Soled (ExxonMobil) for sharing his experiences in synthesis and hydrotreating. ExxonMobil Research and Engineering Company is acknowledged for the financial support of this work.

■ REFERENCES

(1) McVicker, G. B.; Daage, M.; Touvelle, M. S.; Hudson, C. W.; Klein, D. P.; Baird, W. C.; Cook, B. R.; Chen, J. G.; Hantzer, S.; Vaughan, D. E. W.; et al. Selective Ring Opening of Naphthenic Molecules. *J. Catal.* **2002**, *210*, 137−148.

(2) Stanislaus, A.; Cooper, B. H. Aromatic Hydrogenation Catalysis - A Review. *Catal. Rev. Sci. Eng.* **1994**, *36*, 75−123.

(3) Do, P. T.; Alvarez, W. E.; Resasco, D. E. Ring Opening of 1,2-and 1,3-Dimethylcyclohexane on Iridium Catalysts. *J. Catal.* **2006**, *238*, 477−488.

(4) Santikunaporn, M.; Alvarez, W. E.; Resasco, D. E. Ring Contraction and Selective Ring Opening of Naphthenic Molecules for Octane Number Improvement. *Appl. Catal., A* **2007**, *325*, 175−187.

(5) Gault, F. G. Effect de la Dispersion du Platine sur le Support dans L'Hydrogenolyse des Hydrocarbures Cyclopentaniques. *C. R. Acad. Sci.* **1957**, *245*, 1620−1623.

(6) Gault, F. G. Mechanisms of Skeletal Isomerization of Hydrocarbons on Metals. *Adv. Catal.* **1981**, *30*, 1−95.

(7) Maire, G.; Plouidy, G.; Prudhomme, J. C.; Gault, F. G. Mechanisms of Hydrogenolysis and Isomerization of Hydrocarbons on Metals I. Hydrogenolysis of Cyclic Hydrocarbons. *J. Catal.* **1965**, *4*, 556−569.

(8) Shi, H.; Gutierrez, O. Y.; Haller, G. L.; Mei, D.; Rousseau, R.; Lercher, J. A. Structure Sensitivity of Hydrogenolytic Cleavage of Endocyclic and Exocyclic C−C Bonds in Methycyclohexane over Supported Iridium Particles. *J. Catal.* **2013**, *297*, 70−78.

(9) Walter, C. G.; Coq, B.; Figueras, F.; Boulet, M. Competitive Reaction of Methylcyclohexane and n-Hexane over Alumina-Supported Platinum, Iridium, and Ruthenium Catalysts. *Appl. Catal., A* **1995**, *133*, 95−102.

(10) Kramer, R.; Zuegg, H. The Hydrogenolysis of Methylcyclopentane on Platinum Model Catalysts - Particle-Size Effect Due to a

DOI: 10.1021/jp511688x
J. Phys. Chem. C 2015, 119, 2597−2613

Reaction Occurring at the Phase-Boundary Metal Support. *J. Catal.* **1983**, *80*, 446−456.
(11) Samoila, P.; Boutzeloit, M.; Especel, C.; Epron, F.; Marecot, P. Selective Ring-Opening of Methylcyclopentane on Platinum-Based Bimetallic Catalysts. *Appl. Catal., A* **2009**, *369*, 104−112.
(12) Chimentao, R. J.; Valenca, G. R.; Medina, F.; Perez-Ramirez, J. Hydrogenolysis of Methylcyclopentane over the Bimetallic Ir-Au/γ-Al_2O_3 Catalysts. *Appl. Surf. Sci.* **2007**, *253*, 5888−5893.
(13) Poupin, C.; Pirault-Roy, L.; Fontaine, C. L.; Tóth, L.; Chamam, M.; Wootsch, A.; Paál, Z. Promising PtIr, Catalysts for Hydrocarbon Transformation: Comparison of Different Preparation Methods. *J. Catal.* **2010**, *272*, 315−319.
(14) Anslyn, E. V.; Dougherty, D. A. *Modern Physical Organic Chemistry*; University Science Books: Sausalito, CA, 2006.
(15) McMillen, D. F.; Golden, D. M. Hydrocarbon Bond Dissociation Energies. *Annu. Rev. Phys. Chem.* **1982**, *33*, 493−532.
(16) Flaherty, D. W.; Iglesia, E. Transition State Enthalpy and Entropy Effects on Reactivity and Selectivity in Hydrogenolysis of n-Alkanes. *J. Am. Chem. Soc.* **2013**, *135*, 18586−18599.
(17) Flaherty, D. W.; Hibbitts, D. D.; Gürbüz, E. I.; Iglesia, E. Theoretical and Kinetic Assessment of the Mechanism of Ethane Hydrogenolysis on Metal Surfaces Saturated with Chemisorbed Hydrogen. *J. Catal.* **2014**, *311*, 350−356.
(18) Flaherty, D. W.; Hibbitts, D. D.; Iglesia, E. Metal-Catalyzed C-C Bond Cleavage in Alkanes: Effects of Methyl Substitution on Transition-State Structures and Stability. *J. Am. Chem. Soc.* **2014**, *136*, 9664−9676.
(19) Soled, S. L.; Malek, A.; Miseo, S.; Baumgartner, J.; Kliewer, C.; Afeworki, M.; Stevens, P. A. Supported Metal Catalysts: Some Interesting New Leads In An Old Field. *Stud. Surf. Sci. Catal.* **2006**, *162*, 103−110.
(20) McVicker, G. B.; Baker, R. T. K.; Garten, R. L.; Kugler, E. L. Chemisorption Properties of Iridium on Alumina Catalysts. *J. Catal.* **1980**, *65*, 207−220.
(21) Cortright, R. D.; Watwe, R. M.; Dumesic, J. A. Ethane Hydrogenolysis over Platinum: Selection and Estimation of Kinetic Parameters. *J. Mol. Catal. A: Chem.* **2000**, *163*, 91−103.
(22) Watwe, R. M.; Cortright, R. D.; Norskov, J. K.; Dumesic, J. A. Theoretical Studies of Stability and Reactivity of C_2 Hydrocarbon Species on Pt Clusters, Pt(111), and Pt(211). *J. Phys. Chem. B* **2000**, *104*, 2299−2310.
(23) Sinfelt, J. H.; Taylor, W. F.; Yates, D. J. C. Catalysis over Supported Metals. 3. Comparison of Metals of Known Surface Area for Ethane Hydrogenolysis. *J. Phys. Chem.* **1965**, *69*, 95−101.
(24) Sinfelt, J. H.; Yates, D. J. C. Catalytic Hydrogenolysis of Ethane over Noble Metals of Group 8. *J. Catal.* **1967**, *8*, 82−90.
(25) Shi, H.; Li, X.; Haller, G. L.; Gutierrez, O. Y.; Lercher, J. A. Active Site and Reactive Intermediates in the Hydrogenolytic Cleavage of C-C Bonds in Cyclohexane over Supported Iridium. *J. Catal.* **2012**, *295*, 133−145.
(26) Zhao, Z.-J.; Moskaleva, L. V.; Rosch, N. Tuning the Selectivity for Ring-Opening Reactions of Methylcyclopentane over Pt Catalysts: A Mechanistic Study from First-Principles Calculations. *J. Catal.* **2012**, *285*, 124−133.
(27) Zhao, Z.-J.; Moskaleva, L. V.; Rosch, N. Ring-Opening Reactions of Methylcyclopentane over Metal Catalysts, M= Pt, Rh, Ir, and Pd: A Mechanistic Study from First-Principles Calculations. *ACS Catal.* **2013**, *3*, 196−205.
(28) Dokjampa, S.; Rirksomboon, T.; Phuong, D. T. M.; Resasco, D. E. Ring Opening of 1,3-Dimethylcyclohexane on Ir Catalysts Modification of Product Distribution by Addition of Ni and K to Improve Fuel Properties. *J. Mol. Catal. A: Chem.* **2007**, *274*, 231−240.
(29) Bond, G. C.; Cunningham, R. H. Alkane Transformations on Supported Platinum Catalysts - 4. Kinetics of Hydrogenolysis of Ethane, Propane, and n-Butane on Pt/Al_2O_3 (EUROPT-3) and PtRe/Al_2O_3 (EUROPT-4). *J. Catal.* **1997**, *166*, 172−185.
(30) Engstrom, J. R.; Goodman, D. W.; Weinberg, W. H. Hydrogenolysis of Ethane, Propane, and n-Butane on the (111) and (110) - (1 × 2) Surfaces of Iridium. *J. Am. Chem. Soc.* **1988**, *110*, 8305−8319.
(31) Bond, G. C.; Slaa, J. C. Studies on Ruthenium Catalysts. 4. Hydrogenolysis of n-Butane on Ru/Al_2O_3 Catalyst - Dependence of Reaction-Kinetics on Particle Size and on Pretreatment. *J. Mol. Catal.* **1994**, *89*, 221−228.
(32) Zhao, Z.-J.; Moskaleva, L. V.; Rosch, N. Formation of *n*-Hexane from Methylcyclopentane via a Metallacyclobutane Intermediate at Step Sites of Pt Surfaces: Mechanism from First-Principles Calculations. *J. Catal.* **2013**, *299*, 146−149.
(33) Burwell, R. L. The Surface Organometallic Zoo - Continued. *Catal. Lett.* **1990**, *5*, 237−256.
(34) Chakarov, D. V.; Marinova, T. Adsorption and Thermal Decomposition of Ethylene on Clean and Carbon Monoxide-Covered Ir(110) Surfaces. *Surf. Sci.* **1990**, *227*, 297−309.
(35) Hill, J. E.; Shen, J.; Watwe, R. M.; Dumesic, J. A. Microcalorimetric, Infrared Spectroscopic, and DFT Studies of Ethylene Adsorption on Pd and Pd/Sn Catalysts. *Langmuir* **2000**, *16*, 2213−2219.
(36) Herron, J. A.; Tonelli, S.; Mavrikakis, M. Atomic and Molecular Adsorption on Ru(0001). *Surf. Sci.* **2013**, *614*, 64−74.
(37) Yang, M.; Somorjai, G. A. Adsorption and Reactions of C_6 Hydrocarbons at High Pressures on Pt(111) Single-Crystal Surfaces Studied by Sum Frequency Generation Vibrational Spectroscopy: Mechanisms of Isomerization and Dehydrocyclization of *n*-Hexane. *J. Am. Chem. Soc.* **2004**, *126*, 7698−7708.
(38) Mavrikakis, M.; Rempel, J.; Greeley, J.; Hansen, L. B.; Norskov, J. K. Atomic and Molecular Adsorption on Rh(111). *J. Chem. Phys.* **2002**, *117*, 6737−6744.
(39) Valcarcel, A.; Clotet, A.; Ricart, J. M.; Delbecq, F.; Sautet, P. Comparative DFT Study of the Adsorption of 1,3-Butadiene, 1-Butene, and 2-*cis/trans*-Butenes on the Pt(111) and the Pd(111) Surfaces. *Surf. Sci.* **2004**, *549*, 121−133.
(40) Natal-Santiago, M. A.; Podzolkin, S. G.; Cortright, R. D.; Dumesic, J. A. Microcalorimetric Studies of Interactions of Ethene, Isobutene, and Isobutane with Silica-Supported Pd, Pt, and PtSn. *Catal. Lett.* **1997**, *45*, 155−163.
(41) Karp, E. M.; Silbaugh, T. L.; Campbell, C. T. Energetics of Adsorbed CH_3 on Pt(111) by Calorimetry. *J. Am. Chem. Soc.* **2013**, *135*, 5208−5211.
(42) Lytken, O.; Lew, W.; Campbell, C. T. Catalytic Reaction Energetics by Single Crystal Adsorption Calorimetry: Hydrocarbons on Pt(111). *Chem. Soc. Rev.* **2008**, *37*, 2172−2179.
(43) Blanksby, S. J.; Ellison, G. B. Bond Dissociation Energies of Organic Molecules. *Acc. Chem. Res.* **2003**, *36*, 255−263.
(44) Kua, J.; Faglioni, F.; Goddard, W. A. Thermochemistry for Hydrocarbon Intermediates Chemisorbed on Metal Surfaces: $CH_{n-m}(CH_3)_m$ with n = 1, 2, 3, and m < n on Pt, Ir, Os, Pd, Rh, and Ru. *J. Am. Chem. Soc.* **2000**, *122*, 2309−2321.
(45) Ford, D. C.; Xu, Y.; Mavrikakis, M. Atomic and Molecular Adsorption on Pt(111). *Surf. Sci.* **2005**, *587*, 159−174.
(46) Krekelberg, W. P.; Greeley, J.; Mavrikakis, M. Atomic and Molecular Adsorption on Ir(111). *J. Phys. Chem. B* **2004**, *108*, 987−994.
(47) Yaws, C. L. *Yaws' Handbook of Thermodynamic and Physical Properties of Chemical Compounds*; Knovel: New York, 2003.
(48) Chen, Y.; Vlachos, D. G. Hydrogenation of Ethylene and Dehydrogenation and Hydrogenolysis of Ethane on Pt(111) and Pt(211): A Density Functional Theory Study. *J. Phys. Chem. C* **2010**, *114*, 4973−4982.
(49) Fenoglio, R. J.; Nunez, G. M.; Resasco, D. E. Selectivity Changes in the Ring-Opening Reaction of Methylcyclopentane over Rhodium Catalysts Caused by the Addition of Silver and Metal Support Interactions. *Appl. Catal.* **1990**, *63*, 319−332.
(50) Clark, A. *The Theory of Adsorption and Catalysis*; Academic Press: New York, 1970.
(51) McQuarrie, D. A. *Statistical Mechanics*; University Science Books: Sausalito, CA, 2000.

DOI: 10.1021/jp511688x
J. Phys. Chem. C 2015, 119, 2597−2613

(52) Smith, G. D.; Jaffe, R. L. Quantum Chemistry Study of Conformational Energies and Rotational Energy Barriers in *n*-Alkanes. *J. Phys. Chem. B* **1996**, *100*, 18718−18724.
(53) Zimmer, H.; Paal, Z. Reactions of Alkylcyclopentanes over Pt Catalysts. *J. Mol. Catal.* **1989**, *51*, 261−278.
(54) Guil, J. M.; Perez Masia, A.; Ruiz Paniego, A.; Trejo Menayo, J. M. Energetics of H_2 and O_2 Adsorption on Ir/γ-Al_2O_3 and Ir/SiO_2 Catalysts. Dependence on Support and on Metal Particle Size. *Thermochim. Acta* **1998**, *312*, 115−124.
(55) Pankratiev, Y. D.; Buyanova, N. E.; Turkov, V. M.; Shepelin, A. P.; Malyshev, E. M.; Zhdan, P. A. Adsorption Heats of Hydrogen, Oxygen, and Carbon Monoxide on Iridium Catalysts and their Correlation with Surface Chemical Composition. *React. Kinet. Catal. Lett.* **1982**, *20*, 139−144.
(56) van Santen, R. A.; Neurock, M. *Molecular Heterogeneous Catalysis: A Conceptual and Computational Approach*; Wiley-VCH: Weinheim, 2006.
(57) van Hardeveld, R.; Hartog, F. The Statistics of Surface Atoms and Surface Sites on Metal Crystals. *Surf. Sci.* **1969**, *15*, 189−230.
(58) Bej, S. K.; Maity, S. K.; Turaga, U. T. Search for an Efficient 4,6-DMDBT Hydrodesulfurization Catalyst: A Review of Recent Studies. *Energy Fuels* **2004**, *18*, 1227−1237.

DOI: 10.1021/jp511688x
J. Phys. Chem. C 2015, 119, 2597−2613